2018

Regulation of Microvesicle Particle Release in Keratinocytes

Azeezat Afolake Awoyemi
Wright State University

REGULATION OF MICROVESICLE PARTICLE RELEASE IN KERATINOCYTES

A thesis submitted in partial fulfilment of the

Requirements for the degree of

Master of Science

By

AZEEZAT AFOLAKE AWOYEMI

B.S., University of Lagos, 2015

2018

Wright State University

WRIGHT STATE UNIVERSITY

GRADUATE SCHOOL

JULY 23, 2018

I HEREBY RECOMMEND THAT THE THESIS PREPARED UNDER MY SUPERVISION BY **Azeezat Afolake Awoyemi** ENTITLED Regulation of Microvesicle Particle release in keratinocytes. BE ACCEPTED IN PARTIAL FULFILLMENT OF THE REQUIREMENTS FOR THE DEGREE OF **Master of Science.**

Jeffrey B. Travers, M.D., Ph.D.
Thesis Director

Jeffrey B. Travers, M.D., Ph.D.
Chair, **Department of Pharmacology and Toxicology**

Committee on Final Examination

Jeffrey B Travers, M.D., Ph.D.

Ravi Sahu, Ph.D.

Ji Chen-Bihl, M.D., Ph.D.

Barry Milligan, Ph.D.
Interim Dean of the Graduate School

ABSTRACT

Awoyemi, Azeezat Afolake. M.S. Department of Pharmacology and Toxicology, Wright State University, 2018. Regulation of Microvesicle Particle release in keratinocytes.

Microvesicle particles (MVPs) are produced from cellular membranes and are thought to mediate cell-cell communication, including in response to stressors such as UVB radiation and thermal burn injury. Previous studies have shown that stress-induced MVP release requires the platelet-activating factor (PAF) receptor in human keratinocytes and that pharmacological inhibition of acid sphingomyelinase (ASM) blocked this release. To validate a genetic role for ASM in MVP release, we used CRISPR-Cas9 gene silencing in human keratinocytes and primary fibroblasts derived from ASM-knockout mice. Though MVP release was partially blocked in ASM-deficient mouse fibroblasts, the inability to fully knockdown ASM in HaCaT cells resulted in no significant impact on MVP production. We also found that ethanol, which is known to augment PAF production, stimulated MVP release in human keratinocytes and in mice in vivo. These studies therefore provide additional insights into the role of ASM and ethanol in MVP release.

TABLE OF CONTENTS

LIST OF FIGURES

LIST OF TABLES

ACKNOWLEDGMENTS

I would like to thank my mentor Dr. Jeffrey B. Travers, Dr. Michael Kemp, Christine Rapp, Langni Liu, Dr. Eric Romer, Pariksha Thapa, Dr. Ravi Sahu, Dr. Ji Bihl, Dr. Chen's Laboratory, my family, the Wright State University Department of Pharmacology and Toxicology.

Studies funded by NIH R01 HL062996 and VA Basic Merit Grant BX000853

CHAPTER 1: INTRODUCTION

1.1 Statement of Problem

Microvesicle particles (MVPs) play a significant role in pathological processes by transmitting mechanistic signals from secretory cells to recipient cells in both the healthy and disease state. MVPs are potential biomarkers and could be exploited for diagnostic or therapeutic uses. Given that our group's previous studies have provided evidence that various environmental stressors generate MVP in skin keratinocytes, an improved understanding of MVP regulation by the enzyme acid sphingomyelinase and testing the ability of the polar solvent ethanol to modulate release of these subcellular particles are the two problems this project was designed to address.

1.2 Significance

The significance of these studies is that MVPs may play important roles in how keratinocytes respond to environmental stressors. Thus, the regulation of MVP release could provide new targets to treat injuries from UVB and thermal burn. Moreover, our group has implicated the lipid mediator Platelet-activating factor (PAF) in how environmental stressors interact with skin, as well as how ethanol can augment environmental stressor effects. For example, studies have shown that the intoxicated state of people who are exposed to thermal burn result in increased morbidity and mortality that those without prior exposure [1]. Thus, these studies can provide important and clinically-relevant insights into how the skin responds to external stressors.

1.3 Statement of Purpose

The aims of this study are two-fold. First, we will attempt to verify whether the genetic knockout of ASM decreases MVP release upon exposure to thermal burn injury and UVB radiation in keratinocytes. Does treatment of ASM KO cells with C2-ceramide increase MVP? Does treatment of HaCaT cells, WT and PAFR-KO mice with EtOH, burn and EtOH + Burn increase MVP release? Does treatment of HaCaT cells with CPAF cause translocation of ASM from the nucleus to the cell membrane? Does ethanol exposure modulate MVP exposure, either in keratinocytes in vitro or in mice in vivo?

1.4 Hypothesis

Our hypothesis is that the knockout of ASM in mammalian cells will inhibit the production of MVPs upon exposure to stressors in comparison to wild type cells. We also predict the translocation of ASM from the nucleus to the membrane after treatment with CPAF.

We expect that HaCaT cells treated with ethanol and later exposed to thermal burn in a time dependent manner will result in augmented MVP release. We expect that PAFR-KO mice will result in a decreased MVP release in comparison to WT mice upon treatment with ethanol plus thermal burn both from skin as well as in serum.

Null Hypothesis

H_o: $\mu_{Ø} = \mu_C = \mu_U = \mu_B$: The mean release of MVP in group without treatment is equal to the mean release MVP of CPAF, UVB and Burn groups of ASM-KO HaCaT cells

H_a: Not all means of release of MVP are the same.

1. Null Hypothesis

H_o: $\mu_{Ø} = \mu_C = \mu_U = \mu_B$: The mean release of MVP in WT NMF group is equals to the mean release MVP of CPAF, UVB and Burn groups of ASM-KO NMF

H_a: Not all means of release of MVP are the same.

2. Null Hypothesis

H_o: $\mu_{Ø} = \mu_E = \mu_B = \mu_{E+B}$: The mean release of MVP in group without treatment is equals to the mean release MVP of EtOH, TBI and EtOH+ TBI groups of HaCaT cells

H_a: Not all means of release of MVP are the same.

3. Null Hypothesis

H_o: $\mu_{Ø} = \mu_E = \mu_B = \mu_{E+B}$: The mean release of MVP in group of WT mice is equals to the mean release MVP of EtOH, TBI and EtOH+ TBI groups of PAFR-KO mice

H_a: Not all means of release of MVP are the same.

4. Null Hypothesis

H_o: $\mu_{Ø} = \mu_C$: The mean release of MVP in group without treatment is equals to the mean release MVP of CPAF groups of HaCaT cells

H_a: Not all means of release of MVP are the same.

1.5 Research Objectives

- To develop a genetic approach to study the role of ASM in MVP release in response to CPAF, thermal burn injury and UVB irradiation in mammalian cells.
- To determine if EtOH increases MVP release in keratinocytes

- To determine if exposure to EtOH prior to thermal burn injury causes increase in MVP release *in vitro* and *in vivo.*
    - To test if there is increase MVP release systematically on exposure to EtOH and thermal burn injury *in vivo.*
- To test the translocation of ASM to the membrane in keratinocytes upon treatment with CPAF.

1.6 Abbreviations

- ✓ **ASM:** Acid Sphingomyelinase
- ✓ **C2:** C2 Ceramide
- ✓ **CAS9:** CRISPR-associated proteins
- ✓ **CPAF:** Carbamoyl-PAF
- ✓ **CRISPR:** Clustered, regularly interspaced short palindromic repeats
- ✓ **DMEM:** Dulbecco's Modified Eagle Medium
- ✓ **DMSO:** Dimethyl sulfoxide
- ✓ **di- C2:** C2 Dihydroceramide (N-acetoyl-D-erythro-sphinganine)
- ✓ **EtOH:** Ethyl Alcohol (C2H5OH)
- ✓ **gRNA:** guide Ribonucleic Acid
- ✓ **HaCaT:** Human Keratinocyte cell line
- ✓ **HBSS:** Hanks' Balanced Salt Solution
- ✓ **HR:** Homologous Recombination
- ✓ **KO:** Knockout
- ✓ **MVP:** Microvesicle particle
- ✓ **NHEJ:** Non-homologous end joining
- ✓ **NMF:** Normal Murine Fibroblast

- ✓ **PAF:** Platelet Activating Factor
- ✓ **PAF-R:** Platelet Activating Factor Receptor
- ✓ **PAM:** Protospacer Adjacent Motif
- ✓ **PBS:** Phosphate Buffered Saline
- ✓ **ROS:** Reactive Oxygen Species
- ✓ **TBI:** Thermal Burn Injury
- ✓ **UVB:** Ultraviolet B radiation
- ✓ **WT:** Wild Type

1.7 Assumptions

We made the assumption that keratinocytes and fibroblasts respond in the same manner as to when in the whole-body system when exposed to different treatments. In addition, we made the assumption that mice will react the same upon treatment irrespective of the gender of the mice.

CHAPTER 2: LITERATURE REVIEW

2.1 Microvesicle Particles

Microvesicle particles are small spherical shaped particles of 100-1000 nm in diameter [2,3] that bleb directly from the plasma membrane of various cell types such as epithelial cells, neutrophils, tumor cells, macrophages and monocytes [4]. This process might be as a result of the beginning of apoptosis [3,4], upon serum deprivation [5] or activation by internal or external stimuli which causes increases in the level of intracellular calcium and results in MVP release from the plasma membrane [4]. MVPs were earlier referred to as platelet dust [6], but were later shown that they carry various bioactive substances including signalling proteins, bioactive lipids, cytokines, chemokines and nucleic acids, enzymes, and growth factors [3]. On exposure to external stimuli such as TBI, UVB, or cigarette smoke, MVP are thought to contain bioactive substances. Signals are mediated by MVP thus by promptly transferring these biological substances from a parent cell, either in an healthy state or diseased state (MVP shed from cancerous cells may promote spreading of oncogenes) to neighbouring cells and to cells far-off from the parent cell [3].

There are several signalling pathways by which particles can be released and this depends on the trigger agent on the membrane of the cell. For example when an endothelial cell is triggered by thrombin and angiotensin II, the RhOa-ROCK pathway is required [5]. Furthermore, the p38-MAP kinase pathway is needed for particle release when triggered by TNF- α [5] and this process can be blocked by adding inhibitors of the pathways involved in both processes. MVP role in cell to cell communication has

made it a point of interest as a potential tool for therapy, prevention and biomarker of several diseases [3].

2.2 Keratinocyte Damage

Human skin is one of the largest organs in the body, and epidermal keratinocytes have direct regular exposure to environmental and external stressors because they are on the outermost part of the skin. These external stimuli can include ionizing radiation, harmful chemicals, toxins, contaminants and O_3 being the most hazardous [7]. Keratinocytes are largely affected by pro-oxidative stress caused by UV radiation and heat shock [8]. These stressors penetrate the skin barrier causing photo-peroxidation of cellular lipids, production of ROS and damage to cellular DNA [9], which could result in neoplastic tumor formation. Excessive exposure to prolonged oxidative stress can overpower the endogenous protective system consisting of both enzymatic and non-enzymatic processes thus causing damage to the skin [7]. It is essential to both understand the effects of and decrease levels of ROS caused by external factors to avoid perpetual damage to cellular system [8] and production of inflammatory cytokines.

Topical application of resveratrol (a plant polyphenol) can protect the human keratinocyte by inhibiting the formation of cigarette smoke induced ROS and carbonyl development thus acting as a good defensive mechanism [10]. Therapeutic mediation using antioxidants and PAF receptor antagonists is a key approach to lessen the photo-oxidation that occurs upon cutaneous inflammation [9].

2.3 PAF-Receptor

Platelet Activating Factor (1-alkyl-2-acetyl glycerol-phosphocholine) is an inflammatory phospholipid that carries out its action through a G-protein coupled transmembrane receptor, known as PAF-Receptor (PAF-R) that is found on multiple

types of classically immune cells as well as epidermal skin cells [11]. Both PAF and oxidized glycerol-phosphocholines exert agonistic actions on the PAF-R. Pro-oxidative stressors such as jet fuel, chemotherapy agents, cigarette smoke, and UVB all generate ROS that acts upon glycerophosphocholines (GPC) immediately to form oxidized GPC (ox-GPC) which are have strong agonistic effects on PAF-R [12]. Binding of PAF to its receptor activates different second messenger systems, including mitogen-activated kinases, protein kinase C, nuclear factor kappa B pathways, phospholipases, and prostaglandin-generating cyclooxygenase enzymes [13,14]. Activation of this receptor by external stimuli also prompts PAF to be synthesized via enzymatic process indicating a potential feed-forward system [14].

Previous studies have implicated PAF in how keratinocytes generate MVP. PAF agonists generate MVP, and UVB-mediated MVP release requires PAF-R receptor signalling by exposing KBP and KBM cells (KBP cells express the PAF-R but KBM cells do not) to UVB and found that only KBP cells released MVP compared to KBM cells [11]. Thus, that the PAF-R plays a role in UVB-mediated MVP release.

2.3.1 Role of PAF and PAF-R in Keratinocyte Damage

Ultraviolet B radiation (UVB) exerts profound effects on human epidermis and carries out its action by activating bioactive substances and lipids in keratinocytes [14,15] and is a common cause of skin cancer [16]. Stimuli including cytokines, endotoxins and Ca+ ionophores activates rapid PAF synthesis. Keratinocyte damages by thermal burn or cold increments causes an increase in PAF being generated [14]. Epidermal cell exposure to UVB might be a process in which signals are transmitted to

the system [11]. UVB-stimulated acute inflammation enhances the formation of cytokines such as TNF-α [15] and IL-10 [17] through activation of PAF-R. TNF-α formation mediated by UV radiation in epithelial skin cells is linked to inflammation and epidermal cell death has been implicated in UVB-induced inflammation and epidermal cell apoptosis [15]. The PAF system is associated with keratinocyte function and skin inflammatory diseases [18]. PAF-R activation causes production of prostaglandins, IL-8 and COX-2, the latter of which is involved in epidermal carcinogenesis [15,17]. Studies carried out by Yao et al. revealed that antioxidants vitamin C, N-acetylcysteine and the pharmacological inhibitor PD168393 distinctive for the epidermal growth factor receptor blocked UVB-induced ROS and agonists of PAF-R [16].

2.4 Acid Sphingomyelinase

Acid sphingomyelinase is an enzyme involved in catalysing the cleavage of sphingomyelin to ceramide and phosphorylcholine. ASM has an optimum pH of 5.0 [19] and molecular size of 70 kDa [20]. Deficiency of this enzyme has been associated with the rare autosomal recessive disorder Niemann-Pick disease [21] thereby causing skin and neural defects by a pathologic accumulation of sphingolipids in cells and tissues. Earlier studies have shown that ASM is localized in the secretory vesicles on plasma membrane [22]. Upon stimulation, ASM translocates from lysosomal intracellular storage to the outer leaflet of the cell membrane thereby releasing ceramide [23]. Activation of cells triggered by mediating stressors such as PAF, thrombin, amyloid [24], ionizing radiation (IR) [22], by triggering ASM thereby inducing ceramide formation thus causing cell apoptosis and thereby adding to pathophysiology of several diseases. Ceramide can also be produced based on the trigger or type of cell

via a (SMase)-dependent catabolism of sphingomyelin (SM), a de novo synthetic pathway or a salvage synthetic pathway [22].

ASM plays a major role in the secretion of T-lymphocyte granules, degranulation, vesicle blebbing, and MVP release from glial cells [24]. ASM is essential in lipid communication in heart diseases thus causing inflamed vasculature [24]. ASM facilitated ceramide production takes place rapidly and is mainly localized in the plasma membrane [22] thereby stimulating quickly activating cellular functions on activation of the cells [24] and playing a main role in generating pulmonary edema associated with acute lung injury. Studies shows that weak bases prevents ASM activity [19]. Tricyclic anti-depressants such as imipramine, desipramine, and amitriptyline are known to inhibit the function of ASM activity [19] and mitigate receptor-stimulated cell death, apoptosis mediated by cell response to stress stimuli enhance to proliferate due to their anti-cell death effect. Thus, ASM inhibitor may be useful for therapy in diseases such as inflammatory bowel disease and acute lung injury thereby curbing LPS-stimulated inflammatory cytokine release from macrophages [19].

2.4.1 ASM and MVP

Bianco *et al*. proposed a model of P2X7R mediated MVP blebbing processes by the translocation of MVP to the plasma membrane by recruiting ASM activity in glial cells. When the P2X7 receptor is activated, it stimulates the action of ASM via agonism of the P2X7 receptor pathway such as ROCK [25] and p38 MAP kinase activation necessary for MVP formation and release. An important component of MVP shedding is extracellular Ca^{2+} flux which occurs very rapidly [15,16]. A kinetic study of MVP blebbing revealed that they are rapidly released in 5 minutes and

maximal by 20 minutes upon P2X7 receptor activation [26]. Inflammatory cytokines like IL-1β accumulate in MVPs from microglia and are released upon stimulation of P2X7 receptor. The released MVP are involved in cell to cell release of signalling molecules and dissemination of information via several means of secretion and are also known to play an essential role in immune reactions.

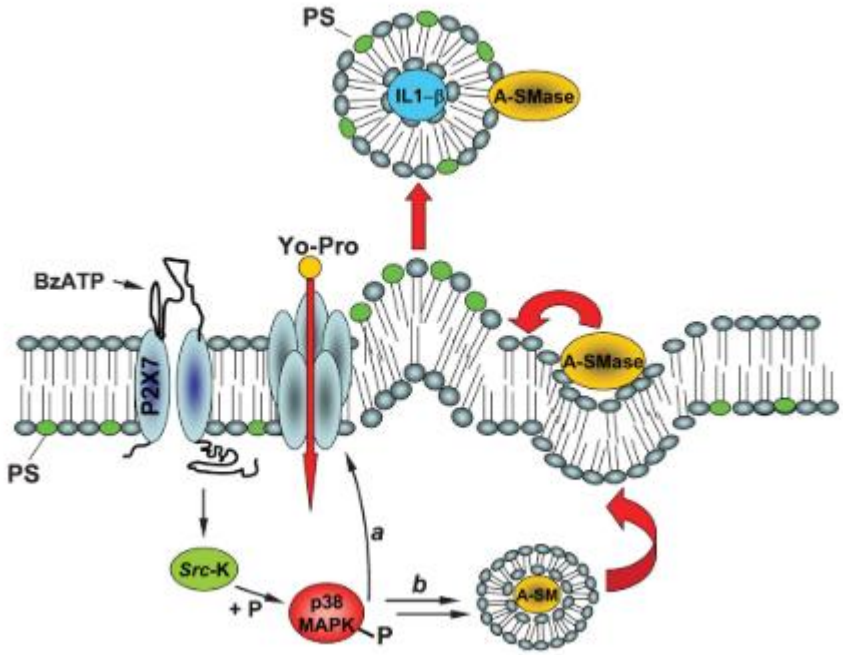

Figure 1: Mechanism of MVP blebbing initiated by activation of P2X7R and engagement of ASM [26].

2.5 Ethanol

One of the most abused substances and leading causes of death worldwide is ethanol (EtOH) [27,28]. Upon exposure to EtOH, ASM activity is activated thereby increasing the level of ceramide [29] and *in vitro* treatment of hepatocytes with EtOH led to a decrease in sphingomyelin and a rise in ceramide levels [30]. Kupffer cells produces TNF-α upon exposure to EtOH, and this cytokine has been identified as a stimuli for ceramide secretion through the stimulation of ASM [31]. Augmented levels

of ASM have been implicated in many pathological conditions including alcoholism [32].

Studies have shown that the treatment of hepatoma cells with EtOH had a major increase in cellular ceramide content by 20% [33]. It has been reported *in vivo* that ASM is activated by EtOH with a resultant increase in the level of cellular ceramide [29]. Treatment of hepatoma cells and mice with EtOH decreased the action and level of AMP Kinase, which is known to control lipid metabolism [18,19] and result in a stimulation of fatty acid synthesis. The phosphorylation of AMP Kinase by EtOH is reported to be overturned using imipramine, thus suggesting that the production of ceramide through ASM is activated by EtOH [33].

2.5.1 Ethanol and TBI

Thermal burn injury is life-threatening health trauma in the world with several cases being reported daily. About 50% of burn patients hospitalized had alcohol in their system when they were exposed to thermal injury and studies revealed that patients with alcohol in their blood stream prior to thermal injury have a 3 to 6-fold increased risk of death [1]. Thermal injury to the skin brings about the degeneration the of lining of intestinal membranes thereby inducing bacterial translocation leading to infections and several organ failure in individuals affected [34]. Prior exposure of individual to alcohol causes higher rate of injury and death. Studies have shown that in mice experiments, ethanol and TBI causes systemic toxicity observed in human having organ failure, acute systemic production and delayed immunosuppression [35].

2.6 Translocation of ASM

ASM is primary located in the nucleus of the cell, however upon exposure to external stimuli such as UV light [36], H_2O_2 [37], *Pseudomonas aeruginosa,* ASM translocates to the outer leaflet of the plasma membrane and is highly dependent on Ca^{2+} levels [37]. It has been shown that lysosomes move and fuse to the plasma membrane in reaction to increased intracellular Ca^{2+} [38]. The method by which Ca^{2+} independently translocates ASM is not well known, but may involve activation of PKCδ by ROS when then interact with vesicles having ASM which is then externalized to the plasma membrane [39]. Confocal analysis of ASM build-up on the surface of the cell was identified as soon as ten minutes of exposure to UVC light and increased at twelve minutes which was reduced to normal level after fifteen minutes as fluorescence signal subsides [36].

2.7 CRISPR CAS9

Clustered Regularly Interspaced Short Palindromic Repeats (CRISPR)-CRISPR associated protein 9 (Cas9) technique, is an effective systemic tool for genetic engineering in biological research which has initiated a new era of genome editing by overcoming the limitations of earlier methods [40]. In 1987, a research group from Japan were the first to illustrate CRISPR in *E. coli* as an odd 29-nucleotide repeat sequence including 32-nucleotide spacing [41].

This systematic tool requires guide RNA (gRNA) which directs the Cas9 endonuclease to the location of double stranded DNA (ds-DNA) sequence of interest to make cuts in the DNA that are then repaired by either NHEJ or HDR-systems to edit the genome [42,43]. Protospacer Adjacent Motive (PAM) helps to modify double

strand break by enabling Cas9 to cut gRNA target to enable a straight transcript recognition in a map out way [44]. HR has been developed to manipulate gene of interest by creating KO and knock-in in vitro and in vivo models [45,46]. On the other hand, NHEJ develops random or by-chance insertion and deletions producing a frameshift mutation, however availability of exogenous donor DNA template around double strand break can repair damage to the DNA through HDR mechanism thereby accurately modifying gene or creating insertion of gene at a point of interest [47].

In the past several years, CRISPR Cas9 has been successfully used in research to modify many different organisms and to develop *in vitro* and *in vivo* models [48,49] and improvement of several diseases in humans. This biological tool has potential in the treatment of sickle cell disease, correcting HBB gene mutation through homologous direct recombination thereby normalizing production of red blood cells [47]. However plenty of work is still required by scientific investigators to solve and eliminate pathogen carrying species such as malaria, Zika virus, and aid drug production [50]. Scientists have successfully demonstrated zebrafish models [51] and in vivo genetic models using CRISPR Cas9.

CRISPR Cas9 technology continues to develop as a potential therapy for use in many genetic disorders through a safe and regulated gene therapy.

CHAPTER 3: Materials and Methods

3.1 Introduction

This chapter discusses the model systems, procedures, and analysis performed to acquire the relevant data to answer the experimental questions of this study. Two model systems were utilized in the studies that were carried out: *in vitro* human and mice cell lines and an *in vivo* mouse model.

3.2 Cells and Cell culture

HaCaT cells are nontumorigenic cells derived from the formation of spontaneously immortalized human skin keratinocytes with its normal epidermal phenotype maintained (1), N-TERTs (telomerase-immortalized normal human keratinocytes), Normal Mice Fibroblasts (NMF) were from the skin of 2-day old WT and ASM-KO mice pups by first removing the epidermis with dispase and then treatment of the dermis with collagenase [53].

3.2.1 Cell growth media and storage condition

Both HaCaT cells and NMF were grown in Dulbecco's modified Eagle's medium, (DMEM Hyclone, Logan, UT) and supplemented with 10% fetal bovine serum (Hyclone, Logan, UT), 100 U penicillin/ 0.1 mg/mL streptomycin (1%), 2 mM glutamine (1%) and incubated at 37°C and 5% CO_2 in a humidified incubator.

3.2.2 Cell passage

Prior growth media were discarded from cells and plates were washed with 1x PBS followed by addition of 2 mL 0.25% Trypsin-EDTA 1X to the HaCaT cells with 10-15 minutes incubation and 2 mL 0.05% Trypsin-EDTA 1X was added to plates containing NMF and incubated for less than 5 minutes in the incubator. After the stipulated time both incubation, 8 mL of growth media was added, cells were resuspended using a 10 mL pipette. Resuspended cells were added to fresh growth media in 10 mL cell culture corning plate at a ratio of 1:10.

3.2.3 Cell count

Cells count was derived from resuspended cells during passage, 200 µL of passaged cells and 800 µL of PBS 1x were added into a 1.5 mL microfuge tube. Cell number was determined using a Millipore Scepter handheld automated cell counter.

3.3 Treatments

2.5 mL of HBSS+ BSA (lipid free) per 10 cm plate to the cells in each treatment group.

Table 1 : Treatment groups

Treatments	Concentration/ Time
No treatment	Ø
Sham	0.1% EtOH
EtOH	1% EtOH
PMA	100 nM

UVB	3.6 KJ/m^2
Thermal burn (90°C)	8s, 45s
CPAF	100 nM

After treatment, HaCaT cells were incubated at in a humidified incubator at 37°C for 4 hours.

3.4 MVP Isolation

On completion of the study design incubation period, 2 mL of the HBSS +BSA was pipetted out from each treatment group into 2 mL microfuge tubes. These were thereby balanced accordingly into Eppendorf® centrifuge 5810R firstly at 2,000 x g for 20 minutes at 4°C. Secondly, after centrifugation was completed, the supernatant was then carefully transferred into new 2 ml microfuge tubes and centrifuged at 20,000 x g for 70 minutes at 4° C. The supernatant was then discarded, and the MVPs were resuspended in 100 µL of filtered 1x PBS. The concentration of MVP was measured with appropriate dilution using Nanoparticle Tracking Analysis (NTA) software version 3.0.

3.5 MVP Analysis

Results obtained from each sample using the NanoSight NTA software version 3.0 were multiplied by the dilution factor to get the concentration, which was then divided by the cell number and multiplied by 100,000 cells. GraphPad Prism was used to graph the result with ANOVA and S.E.M. obtained with a confidence interval of 95 %.

3.6 Mice

C57BL/6 EGFP Wild type mice were obtained from Indiana University–Purdue University Indianapolis (IUPUI) from Dr. Travers colony and were commercially obtained from JAX. Mice were housed together, provided with water and food *ad libitum* in a 12-hour light/dark cycle room. The protocol for experimental use of animals was approved by Wright State University, School of Medicine's Laboratory Animal Care and Use Committee (LACUC).

SMPD1+/- heterozygous mice were obtained from Dr. Irina Petrache's group at National Jewish Medical Center in Denver Colorado. The mice were quarantined and housed together. They were provided with food and water ad libitum in a 12-hour light/dark cycle room. The protocol for experimental use of animals was approved by Wright State University, School of Medicine's Laboratory Animal Care and Use Committee (LACUC). Acid sphingomyelinase knockout mice (SMPD1 -/-), wildtype littermates (SMPD1 +/+) and heterozygous littermates (SMPD1 +/-) were generated and bred. Pups produced were genotyped by polymerase chain reaction (PCR).

PAFR KO mice were obtained from Indiana University–Purdue University Indianapolis (IUPUI) from Dr. Travers colony and were obtained originally from Professor Shimizu from the University of Tokyo. Mice were housed together, provided with water and food *ad libitum* in a 12-hour light/dark cycle room.

All mice were 6-8 weeks old for these studies.

3.6.1 Treatment

Each mouse (WT and PAFR-KO) was weighed and treated in mL/kg according to its weight. The mice were anaesthetized by injecting them with Ketamine/ Xylazine (Intraperitoneally, IP). The mice were shaved on their back using a clipper and

buprenorphine was administered SUB-Q to prevent pain. Experimental groups were sham, EtOH, thermal burn and EtOH + thermal burn. Mice were given EtOH or saline (IP) and 30 min later given thermal burn, as determined by group. The mice were exposed to thermal burn for 8 seconds using a 2 cm by 2 cm stainless steel iron already heated at 90° C in a water bath. Yohimbine was administered to mice to reverse the effects of anaesthesia and given 0.5 mL warm normal saline. The mice were then returned to their individual cages for 2 hour following treatments.

3.6.2 Blood sample collection

After 2 hours, mice were euthanised in a CO_2 tank and cervically dislocated. Blood was then drawn from each mouse using a 1ml 30 g BD- syringe and transferred to an Eppendorf tube. The blood was left to coagulate for 30 minutes and then centrifuged at 15000 g for 15 minutes. The serum (upper clear layer) was then carefully pipetted into a new tube.

3.6.3 Mice skin punch biopsies

Biopsies were taken from mouse skin using 6 mm disposable biopsy punches (Integra Miltex) and were placed in separate Eppendorf tubes. A biopsy from the area of thermal burn and unburnt area (stomach area) was kept in formalin for histology, and other biopsies (3) for MVP analysis and a biopsy stored in RNA later for PCR.

3.6.4 MVP extraction

Five mg/mL collagenase/dispase in 1:1 H_2O was added to each tube needed for MVP analysis. The skin biopsies were then cut into small pieces and left for overnight digestion in a shaker at 37°C. The tissue was then centrifuged at 20,000 x g for 10

minutes, and supernatant was then transferred to a new tube and then centrifuged at 70,000 x g for 10 minutes to remove pellets. Supernatant was transferred to a new tube and centrifuged at 70, 000 x g for 70 minutes. After centrifugation, the supernatant was then discarded, and MVPs were resuspended in 100 µL of filtered 1x PBS. The concentration of MVPs was measured with appropriate dilution using Nanosight (NTA software version 3.0.).

3.6.5 MVP Analysis

Results obtained from each sample using NTA software version 3.0 was multiplied by the rate of dilution to get the concentration, this is then divided by the cell number and multiplied by 100,000 cells. GraphPad Prism was used to graph the result with ANOVA and S.E.M. obtained with a confidence interval of 95 %.

3.7 CRISPR/CAS 9 Knockout of Acid Sphingomyelinase gene

Commercial CRISPR/CAS 9 knockout kits for targeting human ASM were purchased from ORIGENE® The kit had two gRNA vectors, a scramble negative control and a donor vector [54].

3.7.1 Super competent bacterial transformation

Aliquots of competent bacteria stored at -80°C were obtained and thawed on ice. Five ng of donor vector plasmid was added to 50 µL of the competent bacteria and then incubated on ice for 10 minutes. The tube was then placed in a 42°C water bath for 40 sec and transferred back on ice for another 15 minutes. A 2 mL LB was

transferred to a glass tube and the prepared bacteria and plasmid was placed in it and incubated on a shaker at 37 °C for 1 hour 30 minutes. 100 µL of the solution was added to agar plate containing 50 µg/ mL ampicillin spread using a streak plate. It was then incubated overnight at 37°C. The colonies were taken and placed in 120 mL Lysogeny broth (LB) broth containing 100 µg/mL Ampicillin. After this, plasmid DNA was purified using GeneJet kit (Thermo Fisher Scientific).

3.7.2 Enzyme restriction

Agarose gel of 0.4g was weighed and mixed with 40 mL of TAE in a 100 mL conical flask. It was then placed in a microwave until agarose dissolved, then 4 µL of 10 mg/ml ethidium bromide was added, allowed to cool a little, poured into a gel cassette, comb was inserted and allowed to cool.

*Table 2: **Treatment:** gRNA 1& 2 (8022 base pair)*

Label tubes	DNA	NEB buffer 4	PshA1	SacII	PshA1& SacII	H20
PshA1	2µL	1µL	1µL	-	-	6 µL
SacII	2µL	1µL	-	1µL	-	6 µL
PshA1& SacII	2µL	1µL	-	-	1µL	6 µL
Blank	2µL	1µL	-	-	-	7 µL

*Table 3: **Treatment:** pCas-scramble (8022 base pair)*

Label tubes	DNA	NEB buffer 3	PshA1	SacII	PshA1 & SacII	H20
PshA1	2μL	1μL	1μL	-	-	6 μL
SacII	2μL	1μL		1μL	-	6 μL
PshA1 & SacII	2μL	1μL	-	-	1μL	6 μL
Blank	2μL	1μL	-	-	-	7 μL

Table 4: ***Treatment:*** *Donor Plasmid (7020 base pairs)*

Label tubes	DNA	NEB buffer 3	PshA1	SacII	PshA1 & SacII	H20
PshA1	2μL	1μL	1μL	-	-	6 μL
SacII	2μL	1μL		1μL	-	6 μL
PshA1 & SacII	2μL	1μL	-	-	1μL	6 μL
Blank	2μL	1μL	-	-	-	7 μL

2 μL of bromophenol blue (6x) was then added to each tube. 6 μL of these solutions was the loaded into electrophoresis tank and run for 50 mins at 100 volts. The gel was then visualized under UV light using DNA gel viewer.

3.7.3 Cell seeding and Co-transfection

HaCaT cells were seeded in a 6-well plate and allowed to reach confluency of 50-70%. Co-transfection of both gRNAs and donor plasmid was carried out in in duplicate in 6 separate wells and utilized according to the Lipofectamine™ 3000 Reagent protocol from Thermo Fisher. On completion of this, the cells were incubated for 2-4 days at 37 °C.

3.7.4 Cell passaging and colony selection

Forty-eight hours post-transfection, cells were passaged at a ratio of 1:10 and allowed to grow every 3 days after passaging 7 times so as to dilute cells with episomal donor vectors. On the 8th passage, cells were split into a 20 cm dish for colony selection using puromycin selection. The cells were selected with puromycin (2 µg/ml) for 5 days and media was changed every 2-3 days until well separated colonies were formed.

3.7.5 Analysis

Single colonies formed were selected from the 20 cm plates and then expanded. Western blotting and immuno-dot blot assays were carried out to analyse genomic editing results to determine and identify knockout of ASM in each selected colony.

3.7.5.1 Western blot

Growth media was discarded, and cells were washed with cold 1x PBS. Cells from selected colonies were scrapped from culture plates and then RIPA buffer containing protease inhibitor cocktail was added and incubated at room temperature for

30 minutes with shaking at intervals. The samples were then centrifuged at 16,000 x g for 15 minutes, and supernatants were transferred to a new tube. BCA assay was carried out to determine the protein concentration and then 30 µg of proteins was separated by 10% SDS PAGE run at 130 volts for 50 minutes. The proteins were then transferred onto a nitrocellulose membrane using a semi-dry blot transfer for 35 minutes. The membrane was blocked using 5% non-fat dry milk for 1 h and washed with 1x TBST 4 times for 5 minutes each. Membrane was probed with anti-ASM antibody (LifeSpan BioSciences, Inc) (1:2000) overnight, and then with goat anti-rabbit antibody (1:10000) conjugated with HRP for 1 h. ASM bands were detected using SuperSignal West Femto Maximum Sensitivity Substrate (Thermo Fisher scientific) and the images were taken with BioRad imaging system. The membrane was later stripped using a stripping buffer, incubated at 80 °C for 5 minutes, washed, blocked and re-probed using anti-β-actin antibody overnight, as a loading control.

3.7.5.2 Immuno-dot blot assay

To lyse the cells, media from 96-well plate were poured off into a large beaker in the hood and 100 µl of PBS was added to each well of the 96-well plate to briefly rinse the cells. Trypsin-EDTA (40 µl of 0.25%) was added to each well of the 96-well plate and incubate plated in the 37°C incubator until the cells rounded up and began coming off the plate. Cell culture medium (160 µl) was then added to each well of the 96-well plate. The cell suspension was transferred to a new 96-well, clear, flat-bottom, non-sterile plate. Add 100 µl culture medium to the remaining cells and place back into the incubator (cells will re-attach and start to proliferate). Spin the 96-well plate in a swinging bucket rotor for 5 min at 1500 rpm to pellet the cells. Then, pour off the media

from the plates. Next, we added 100 µl of cold PBS to each well of the plate to rinse the cells and spin again for 5 min at 1500 rpm to pellet the cells. 40 µl of RIPA buffer was added to each well of the plate. We next incubated the plate on ice for 10 min and occasionally tap the side of the plate to facilitate cell lysis. We next added 160 µl of cold PBS to each well of the plate and spin the plate at 3250 rpm (max speed) for 5 min. Then transfer the 200 µl soluble lysate to a new 96-well plate.

For protein immunoblotting, we cut a piece of nitrocellulose membrane to the same size as the Bio-Dot SF filter paper (Bio-Rad #1620161) and soaked the nitrocellulose membrane and two pieces of Bio-Dot SF filter paper in 1X PBS. Next, we assembled the dot blot apparatus and tightened the screws and used the vacuum to draw any PBS down from the membrane. Next, we turned off the vacuum and removed the flask plug to release the pressure and completely stop the vacuum. Next, we loaded 200 µl of PBS into each well of the dot blot apparatus. Next, 100 µl of cell lysate was added to the appropriate well. Vacuum (not at full pressure) was used to draw the lysate down through the membrane. After turning off the vacuum and we removed the flask plug and added 200 µl of PBS to each well to wash the membrane and then used the vacuum to draw the PBS through the membrane. We disassembled the dot blot apparatus and carefully remove the nitrocellulose membrane and place on a piece of dry filter paper. Place the membrane into the -80°C incubator for 30 min to dry the membrane. The membrane was wetted with water and then stained with Ponceau dye. Excess dye off was rinsed off with water and then we took a picture of the Ponceau-stained membrane and washed the membrane 3-4 times with TBST to completely remove the Ponceau dye. We then blocked the membrane for 30 min in 5% milk in TBST and was probed with Anti-ASM antibody.

3.7.5.3 MVP release

HaCaT cells systematically edited using CRISPR Cas9 were also analysed by MVP release upon exposure to stressor as follows:

Table 5: Treatment of CRISPR Cas9 edited cells for MVP analysis

Treatments	Concentration/ Time
Sham	Ø
Vehicle	DMSO
CPAF	100 nM
C2-ceramide	20 μM
Dihydroceramide	10 μM
UVB	3.6 KJ/m2
Thermal burn (90°C)	8 secs

After 4-hour incubation time, supernatant was collected for each group.

3.7.5.4 MVP Isolation and Analysis:

MVPs were isolated and quantified as described above.

3.8 Flow cytometry

Cells were treated with or without CPAF and fixed for 10 minutes in 4% paraformaldehyde (w/v) in PBS. The cells were washed using cold 1x PBS and then blocked using 1% BSA for 30 minutes. The cells were washed and incubated with rabbit polyclonal ASM antibody in 1:50 in PBS for 45 minutes. This was followed by washing

the cells and incubating with FITC-labelled goat anti-rabbit secondary antibody for 45 minutes. The cells were washed and analysed using BD accuri C6 flow cytometer system (BD Biosciences).

3.9 Determining the genomic targeting efficiency of Cas9/gRNA with T7 Endonuclease

Genomic DNA from transfected cells were purified with Qiagen genomic DNA purification kit and DNA concentration was measured using PicoGreen quantification protocol adapted for Quant-iT PicoGreen kit.

Forward Primer: GACTCCTTTGGATGGGCCTG

Backward Primer: CTACAATCCATCACTGAGTTTGCTC

Table 6: PCR conditions

Initial duration	94°C	1 min
35 cycles		
Denaturation	94°C	30 sec
Annealing	55°C	30 sec
Extension	72°C	1 min
Final extension	72°C	7 min
Hold	4°C	

50 µl PCR was set up accordingly and PCR conditions used a PCR thermocycler (Thermo Fisher Scientific). The PCR product was purified using PCR purification kit (Invitrogen). The DNA concentration was again quantified with PicoGreen. T7 Endonuclease 1 digestion reaction was set up for denaturation/hybridization using 200

ng DNA, 2 µL 10X NEBuffer2 and the final volume was brought up to 19 µL using distilled DNase free water then put in a thermocycler at stated condition (from NEB website). 1 µL of T7 Endonuclease 1 was added to the PCR products and was incubated for 15 minutes at 37 ^{O}C. The reaction was stopped by adding 0.75 µL of 0.5 M EDTA. 4 µL of 6X loading dye was added to the PCR product and ran on 2% agarose gel stained with ethidium bromide.

3.10 ASM translocation

3.10.1 Cell seeding

Growth media was added to 6-well plates and sterilized glass cover slip was added to each well using sterilized forceps. HaCaT cells added in a ratio 1:100 to growth media, incubated for 1-2 days to attach and grow on the glass cover slip.

3.10.2 Treatment

The cells were treated with or without CPAF and incubated for either 10 or 30 minutes, primary antibody alone and secondary antibody only.

3.10.3 Immunofluorescence

Upon completion of duration of incubation, cells on the cover slips were rinsed briefly in 1x PBS containing 0.1 Triton X- 100. The cells were fixed using 4% paraformaldehyde in 1x PBS for 10 min at room temperature and washed using cold 1x PBS three times. Each cover slip was then blocked to prevent nonspecific binding of antibodies using Normal Horse Serum (Jackson ImmunoResearch) in ratio 1:50 to 1x

PBS for 30 minutes in a humidifying chamber at room temperature. It was then washed, and cells were incubated in primary antibody Anti-ASM antibody at a ratio of 1:100 and incubated for 1 h at room temperature. Cells were washed and incubated using secondary FITC-anti Rabbit at a ratio of 1:100 in the dark for 30 minutes. The cells were then washed with cold PBS three times and a drop of mounting medium conjugated with DAPI was added to microscope slide and the glass cover slips were mounted and images were taking using Cytation 5 Cell Imaging Multi-Mode Reader (BioTek) and then stored in the dark.

CHAPTER 4: RESULTS

4.0 *In vitro* studies

4.1 Dose response effect of ethanol mediated MVP release in HaCaT cells

To determine the dose response effect of EtOH on HaCaT cells, different doses of EtOH (0.1, 0.5, 1, 2.5 and 5%) were used treat keratinocyte cells and were incubated at 37°C for 4 hours (Figure 2). As shown in Figure 2, HaCaT cells responded to exogenous EtOH with increased levels of MVP over baseline levels. Figure 3 shows phase contrast images of HaCaT cells and increased dose of EtOH at 2.5 and 5% treatment was toxic to the keratinocyte cells.

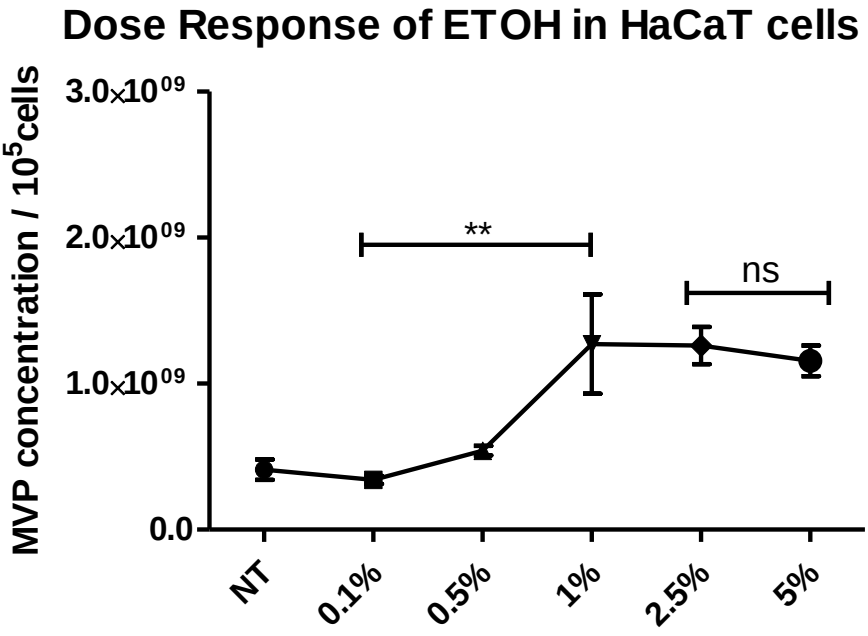

Figure 2: Dose response of EtOH in keratinocyte HaCaT cells

HaCaT cells had either no treatment (NT), or 0.1%, 0.5%, 1%, 2.5% and 5% EtOH. Cells where then incubated for 4 hours. The data represented are mean ± SEM MVP concentration per 100,000 cells (average from 3 independent experiments, n=6). Groups were compared using one-way ANOVA. Differences in samples were considered significant if the P value was less than 0.05. P<0.05 (*), P<0.01 (**), and P<0.001 (***).

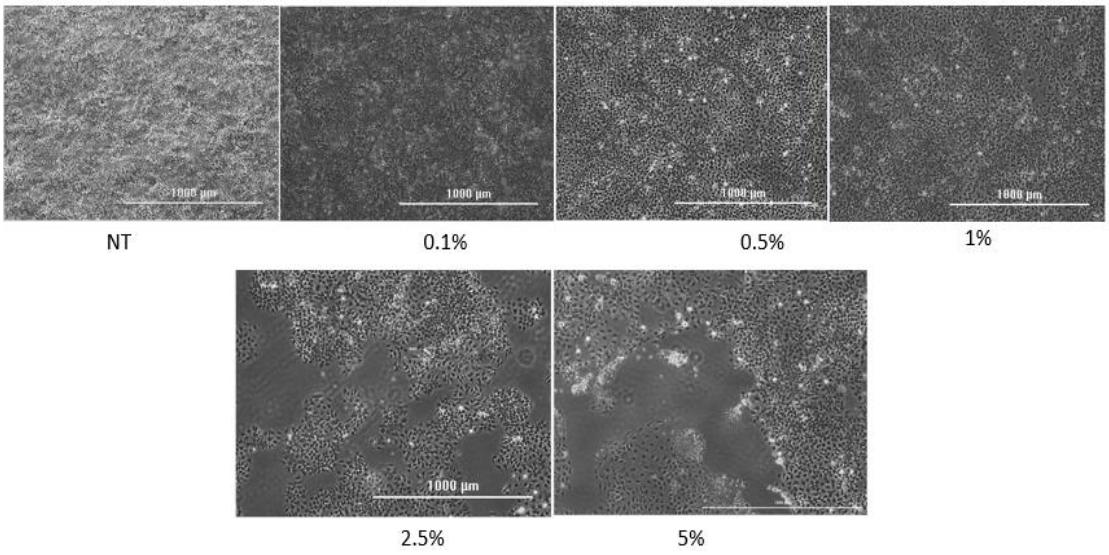

Figure 3: Phase contrast images of the dose response of EtOH treated Keratinocytes

Phase contrast images taken using Cytation 5 Cell Imaging Multi-Mode Reader (BioTek) showed toxicity to the cells as cell lift-off cell culture plates with an increase in level of EtOH after 2 hours.

4.2 EtOH induced MVP release in NTERTs and Normal Human Fibroblasts

The next studies sought to define if other cell types found in skin would respond to exogenous EtOH with increased MVP release. To that end, NTERT cells and Normal Human Fibroblasts (NHF) were treated with 1% EtOH (Figures 4 and 5

respectively) to determine the concentration of MVP release in both cell lines. These studies suggest that HaCaT cells are not unique in responding to exogenous EtOH with increased levels of MVPs.

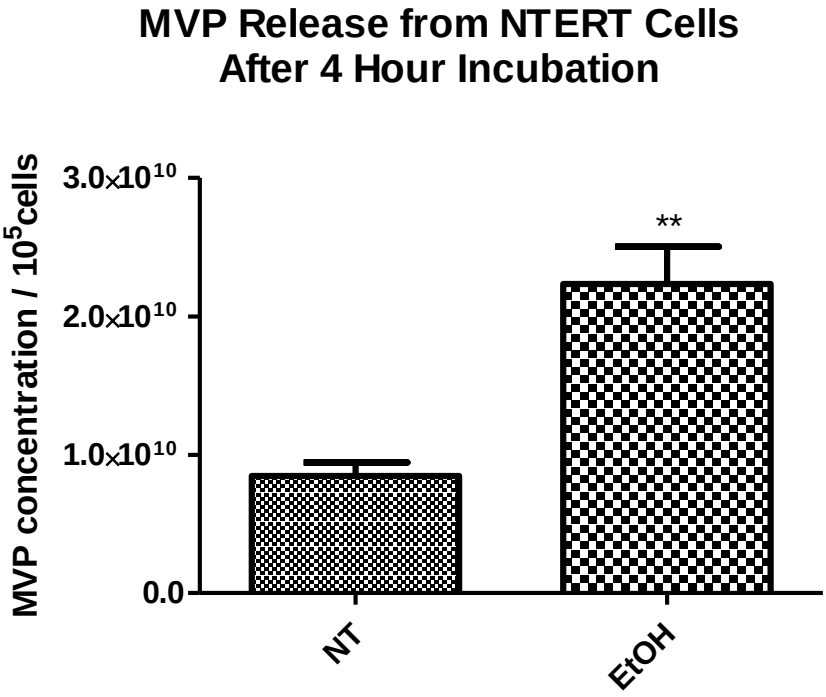

Figure 4: MVP release in NTERT cell on treatment with 1% EtOH

NTERT cells had either no treatment (NT), or 1% EtOH and cells where then incubated for 4 hours. The data represented are mean ± SEM MVP concentration per 100,000 cells (number of samples in each group, n=4). Groups were compared using an unpaired t-test. Differences in samples were considered significant if the P value was less than 0.01 (**).

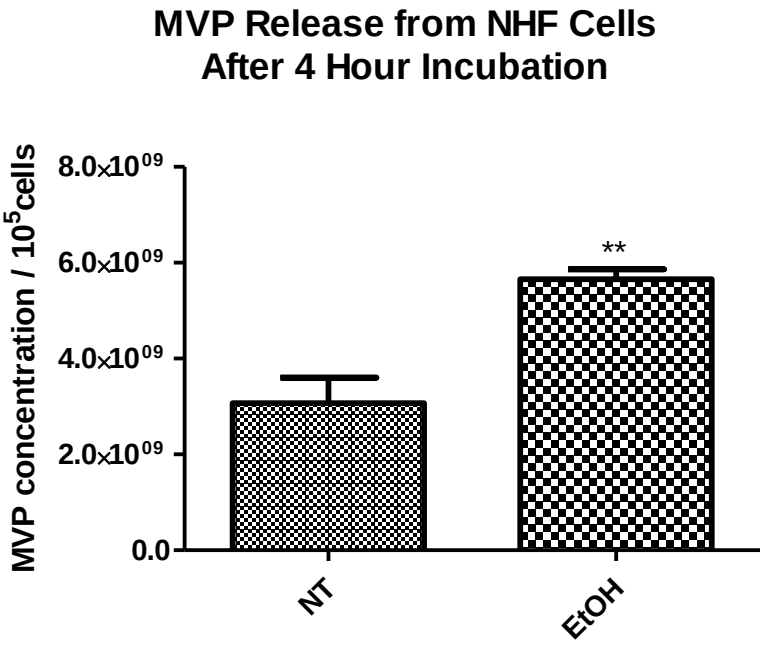

Figure 5: MVP release in Normal Human Fibroblast (NHF) cell on treatment with 1% EtOH

NHF cells had either no treatment (NT), or 1% EtOH and cells where then incubated for 4 hours. The data represented are mean ± SEM MVP concentration per 100,000 cells (number of samples in each group, n=4). Groups were compared using unpaired t-test. Differences in samples were considered significant if the P value was less than 0.01 (**).

4.3 MVP release from HaCaT cells after exposure to EtOH and TBI

The next studies sought to define if combining EtOH and TBI could result in augmented MVP release. As shown in Figure 6, HaCaT cells treated with 1% EtOH generated increased levels of MVP. Moreover, thermal burn injury for 8 and 45 sec induced MVP release at 4h compared to no treatment. Importantly, combining EtOH and TBI resulted in increased levels of MVP release as compared to EtOH or burn

treatments alone (Figure 6). These studies suggest that EtOH can augment burn injury-mediated MVP release. The amounts of MVP appear additive from the individual stimuli.

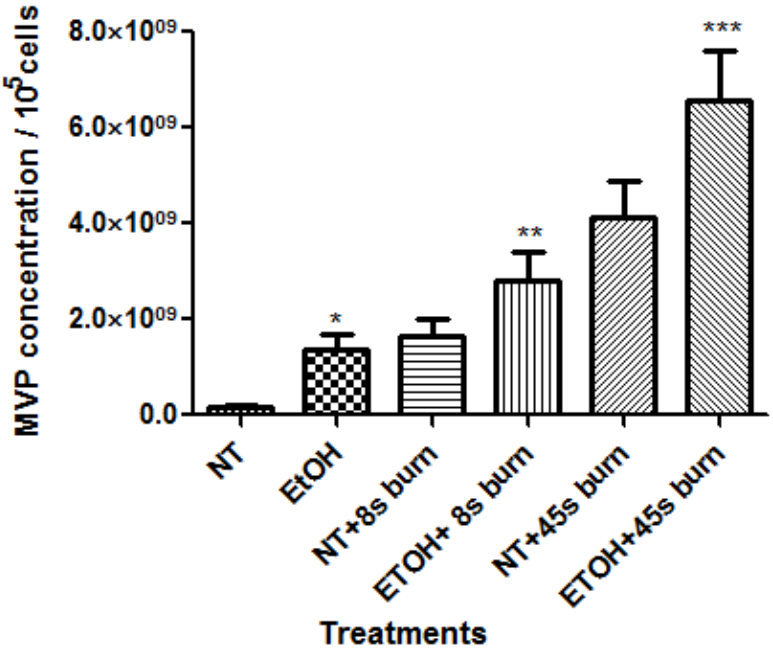

Figure 6: MVP release from HaCaT cells upon exposure to ethanol and burn

HaCaT cells had either no treatment (NT), or 1% EtOH for 30 min followed by 8 and 45 second thermal burn injury. Cells where then incubated for 4 hours. The data represented are mean ± SEM MVP concentration per 100,000 cells (average from 3 independent experiments). Groups were compared using one-way ANOVA. Differences in samples were considered significant if the P value was less than 0.05. P<0.05 (*), P<0.01 (**), and P<0.001 (***).

4.3.1 Effect of imipramine on EtOH- and TBI-induced MVP release in HaCaT cells

To determine whether the pharmacologic ASM inhibitor imipramine will attenuate EtOH and EtOH + TBI induced MVP release, HaCaT cells were treated with or without imipramine (Figure 7). Imipramine did not have a significant effect on EtOH-induced MVP release. However, imipramine significantly decreased MVP release when exposed to EtOH + TBI. These studies suggest the possibility that imipramine modulates MVP release in response to TBI but not EtOH.

.

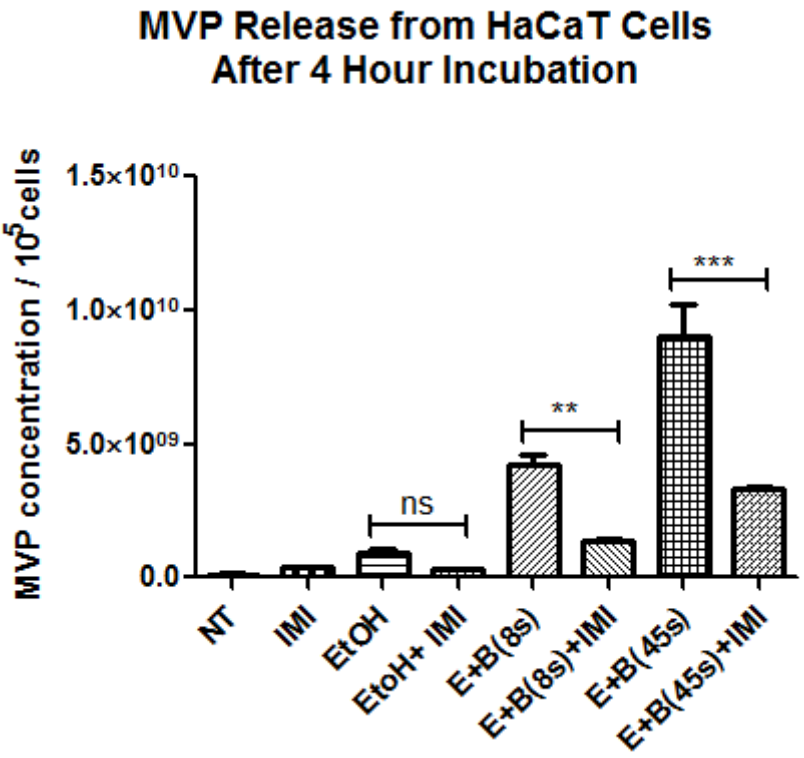

Figure 7: Imipramine blocks MVP release

HaCaT cells were either exposed to no treatment or imipramine for 30 minutes. Cells were then exposed to media alone or 1% EtOH for an additional 30 min. Cells were then treated with TBI as previously outlined. Cells were then incubated for 4 hours. The data represented are mean ± SEM MVP concentration per 100,000 cells (average

from 2 independent experiments). Groups were compared using one-way ANOVA. Differences in samples were considered significant if the P value was less than P<0.01 (**), and P<0.001 (***) and ns denotes no significant.

4.4 Effect of EtOH and UVB on MVP release

We also tested the effect of EtOH and UVB (3,600 J/m^2) on HaCaT cells (Figure 8). There is a significant increase in UVB- or EtOH-induced MVP release, but no significant increase in MVP release was found in combining EtOH + UVB compared to UVB alone.

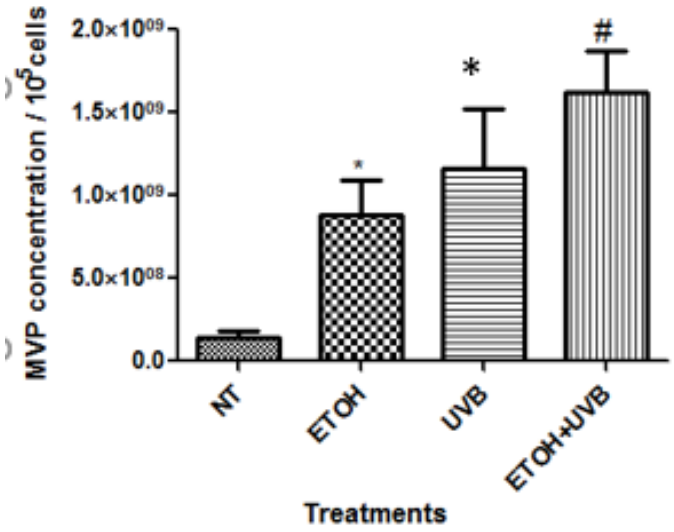

Figure 8: MVP release from HaCaT cells upon exposure to EtOH and UVB

HaCaT cells underwent either no treatment (NT) or 1% EtOH for 30 minutes. The cells were then treated with our Philips UVB source for 12 minutes (3600 J/m^2). Cells where then incubated for 4 hours. The data represented are mean ± SEM MVP concentration per 100,000 cells (average from 2 independent experiments). Groups

were compared using one-way ANOVA. Differences in samples were considered significant if the P value was less than 0.05. P<0.05 (*), and # denotes no significant.

4.5 EtOH stimulates the release of MVPs *in vivo*

To test the effect of EtOH induced MVP release *in vivo*, WT and PAFR-KO mice were utilized to observe the effects of combining TBI and EtOH on keratinocyte and systematic release of MVP from epithelial cells, and role of the PAFR. Using a previously published model [1], mice were treated IP with 20% EtOH and exposed to thermal burn injury for 8 seconds on their back. Burn skin samples were compared to NT skin (Figure 9). Skin biopsies were taken, and cardiac perfusion was done to collect blood. MVP from analyzed punch biopsies showed that WT mice had a significant MVP release on after exposure to TBI and E+TBI compared to skin biopsies taken PAFR KO mice (Figure 10). Furthermore, serum from treated WT mice was significant when mice were treated with ethanol, burn and E+B (Figure 11). Collectively, these experiments suggest that TBI of intoxicated mice results in increased levels of MVP in both skin and serum. Moreover, this effect appears to be dependent upon the PAFR.

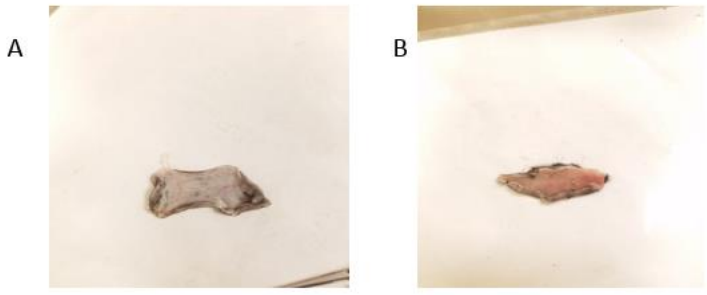

Figure 9: Image of murine back skin treated with TBI

The figure above are skin from A) NT and B) thermal burnt skin WT mice. There is profound redness or inflammation seen in the latter than the former.

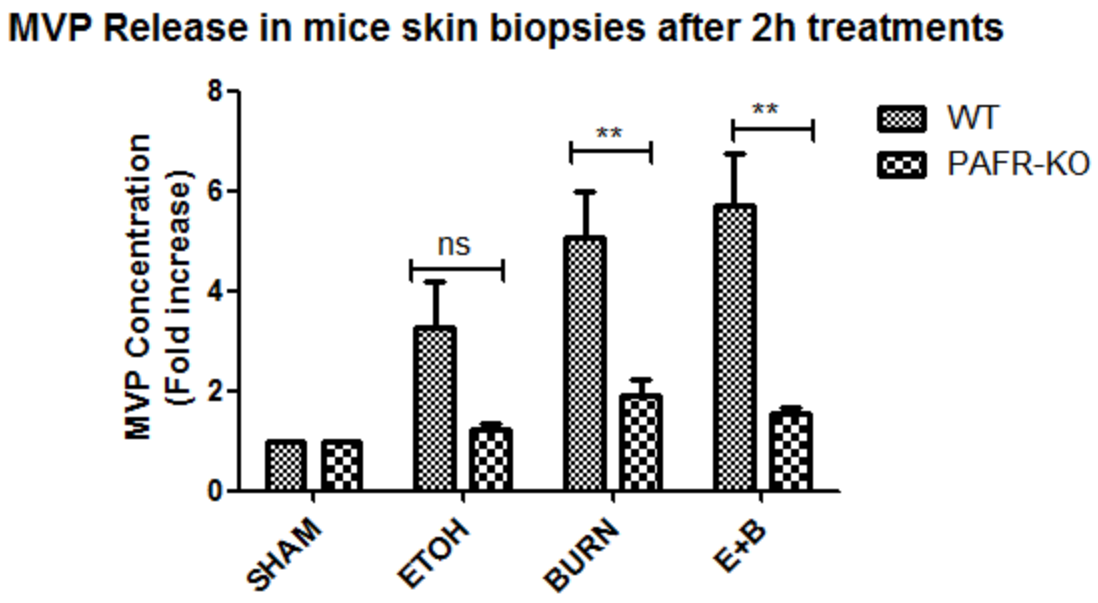

Figure 10: MVP release in murine skin biopsies after 2h treatments

MVP release from WT and PAFR-KO mice punch skin biopsies were measured and analysed using NTA software version 3.0. The data above are mean ± SEM MVP concentration (representative of skin biopsies from 6 mice, from 3 separate experiments). Groups were compared using one-way ANOVA. Differences in samples were considered significant if the P value was less than P<0.01 (**), ns denotes no significance.

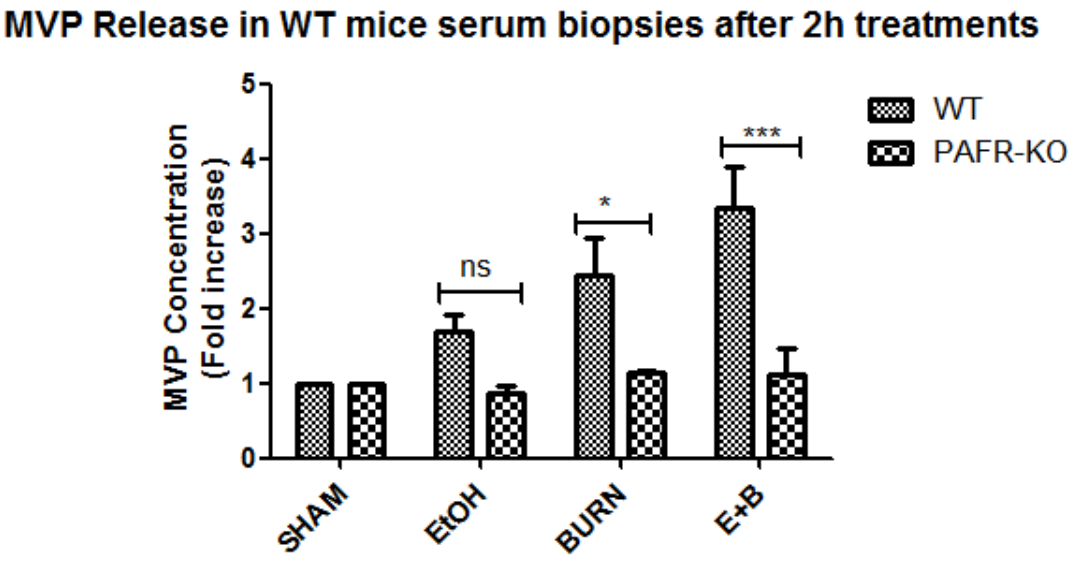

Figure 11: MVP release in mouse sera following EtOH exposure and TBI

MVP release into WT and PAFR-KO mice serum from the experiment outlined in Figure 10 were measured and analysed using NTA software version 3.0. The data above are mean ± SEM MVP (representative of serum from 6 mice, from 3 separate experiments). Groups were compared using one-way ANOVA. Differences in samples were considered significant if the P value was less than 0.05. P<0.05 (*), P<0.001 (***), and ns denotes no significance.

4.6 ASM translocation

To determine whether ASM was targeted to the plasma membrane in response to cell stress, HaCaT cells were treated with CPAF for a duration of 10 and 30 minutes and then ASM localization was determined by indirect immunofluorescence microscopy (Figure 12). Cells stained after a 10-minute exposure showed what could be a potential early formation of ASM on the plasma membrane. In contrast, ASM

staining in the vehicle-treated cells was not well-defined. After 30 minutes of treatments, the fluorescence from the stained cells in both groups decreased.

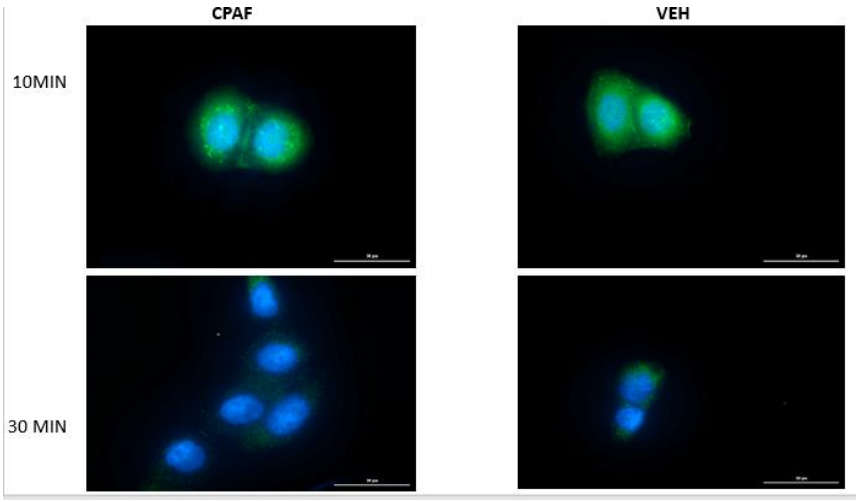

Figure 12: Translocation of ASM to the plasma membrane

HaCaT cells were treated with CPAF or veh (0.1% EtOH) and stained for ASM. Images were taken using Cytation 5 Cell Imaging Multi-Mode Reader (BioTek). ASM is indicated in green and DNA in blue.

4.7 Analysis of potential ASM-KO HaCaT cells

The next studies were designed to create a model of HaCaT cells which lack ASM expression. This novel model could have use in determining if ASM knockout using CRISPR/Cas9 will suppress the PAF system-dependent release of MVP upon exposure to UVB, EtOH, thermal burn injury in the HaCaT- keratinocyte cell line. These studies are critical to confirm findings generated using the pharmacologic inhibitor imipramine. Transfected colonies were screened using immunoblot and MVP release analysis. To show whether ASM expression is absent in selected clones of HaCaT cells

transfected with ASM guide RNAs G1 and G2, Western blot was carried out (Figure 13). For HaCaT, three selected clones from G2, one G1 and HaCaT cells were used as a positive control. ß-actin was the loading control for each lysate. As shown in Figure 12, G25B and G25A had only a partial reduction in ASM protein expression. The graph shows relative ASM protein expression normalized to actin. Immuno-dot blot was carried out by screening 96 different clones (Figure 14). The figure showed that all clones still expressed ASM protein.

.

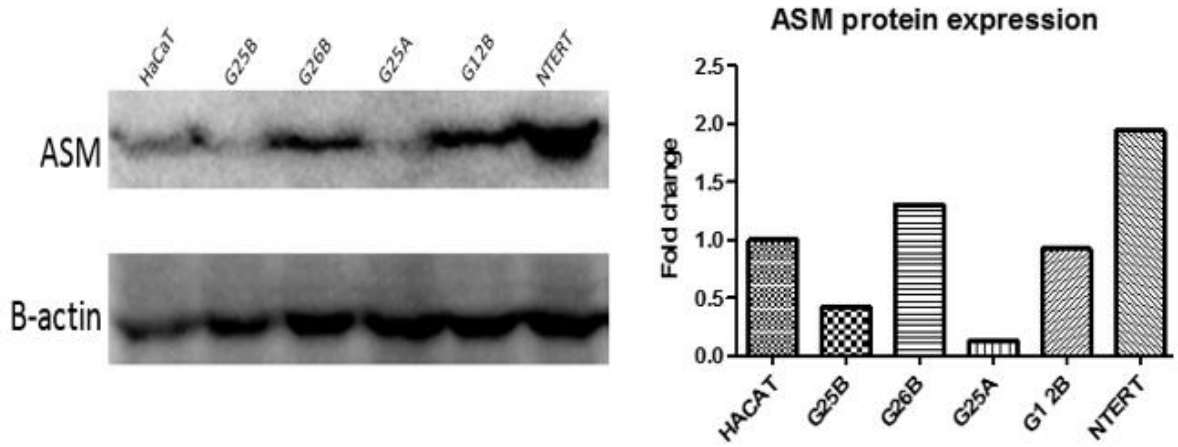

Figure 13: Western blot analysis of ASM expression in keratinocytes and selected colonies

Western blot screening of colonies showing expression of ASM protein. Four different puromycin-resistant clones were analysed using their proteins lysates following transfection with G1 and G2 Guide RNA and CRISPR-Cas9 genome editing. In the graph, the ASM protein was normalized to actin.

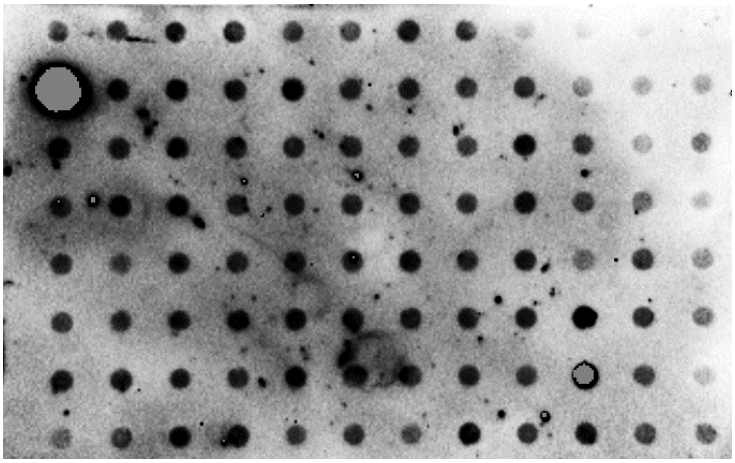

Figure 14: Immuno-dot blot analysis of ASM expression in 96 selected colonies

Immuno-dot blot analysis of CRISPR Cas9 transfected cells. Ninety-six individual clones were screened for ASM protein expression.

4.8 MVP analysis of potential ASM-KO cells.

HaCaT cells were used as a positive control to compare the release of MVP in potential ASM-KO cells, G12B and G25A (Figure 15 and Figure 16). The treatment had 7 groups, NT, Vehicle (DMSO), CPAF, UVB, BURN, C2- ceramide and di-C2. It was observed that the basal level of G1 was lower compared to WT. UVB, treatment caused increase MVP release. Exogeneous C2-ceramide also increase MVP release since ceramide is essential for budding of MVP from plasma membrane. However, BURN and di-C2 treatment caused greater MVP release in comparison to the basal G1. However, G2 (as shown in Figure 13) responded to all treatments thus releasing MVP in comparison to HaCaT.

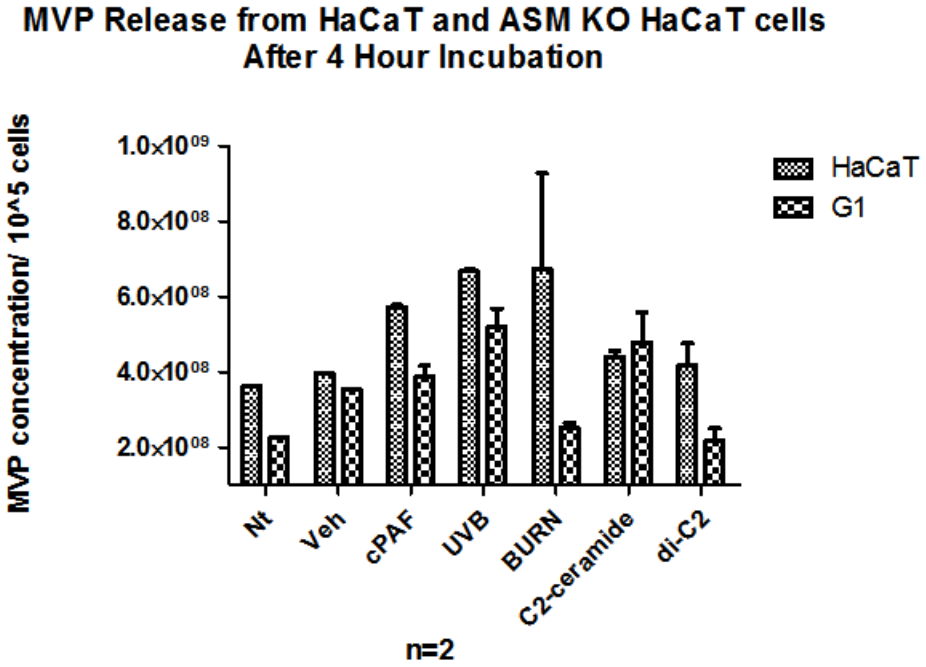

Figure 15:MVP release from HaCaT and ASM KO HaCaT (G1) cells

The ASM gRNA 1 (G1)-transfected cell line G25A had a lower basal level of MVP release, but still responded to UVB exposure and thermal burn injury. The data depicted are mean ± SEM MVP concentration per 100,000 cells.

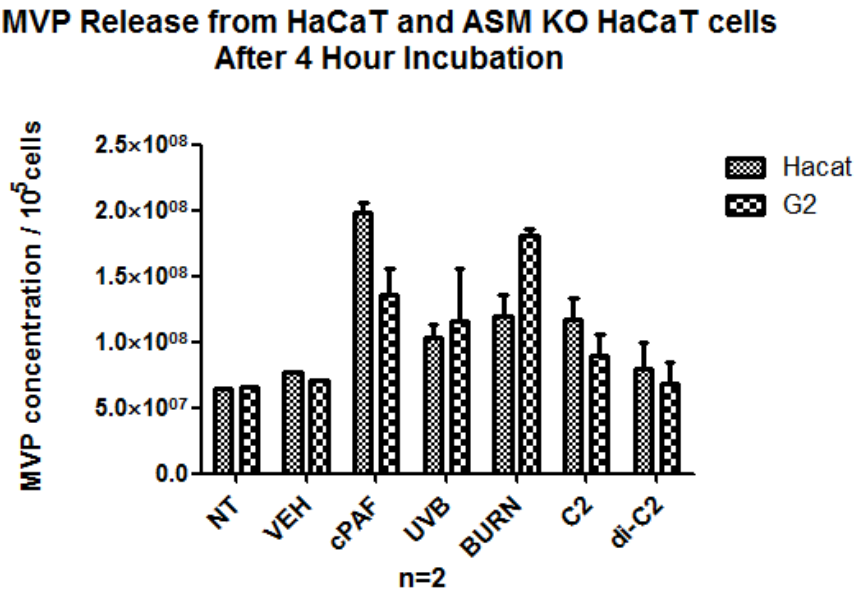

Figure 16: MVP release from HaCaT and ASM KO HaCaT (G2) cells

MVP release from gRNA 2 (G2) (pooled from figure2 G25B) transfected cells responded to UVB and thermal burn on exposure. The data depicted are mean ± SEM MVP concentration per 100,000 cells.

4.9 Flow cytometry

To detect ASM in the plasma membrane upon exposure of HaCaT and potential ASM-KO cells to CPAF and UVB. On exposure to stressors, we identified that both HaCaT and G1 had similar florescence intensity (Figure 17), thus suggesting that ASM is still present in HaCaT cells transfected with G1 gRNA (pooled from Figure 13) targeting ASM.

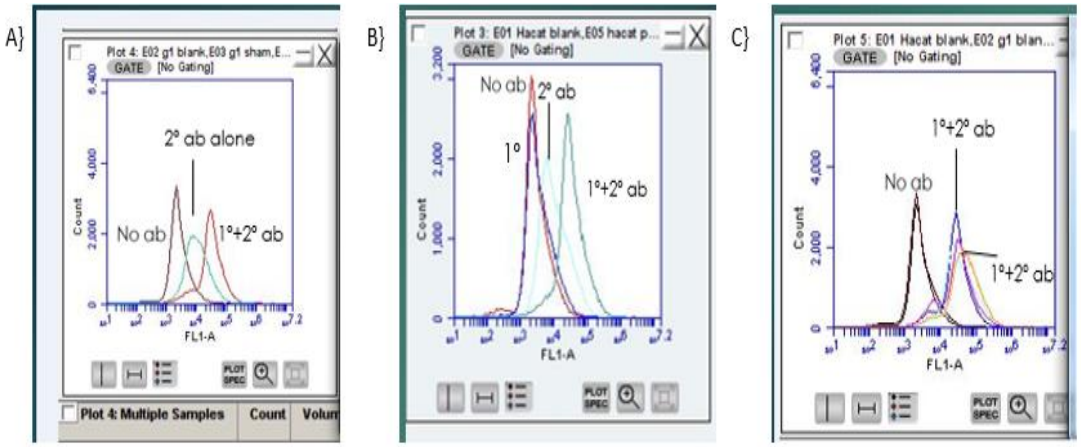

Figure 17: Flow cytometry analysis of ASM fluorescence intensity in HaCaT and G1 cells

Images A &B shows the detection of FITC-stained ASM in G1 and HaCaT cells with no antibody (ab), secondary antibody alone and primary and secondary ab. Image C

shows the combination of both G1 and HaCaT cells treated with no ab, CPAF and UVB.

4.10 Determining genomic targeting efficiency of Cas9/gRNA with T7 Endonuclease 1

To determine the Cas9 targeting efficiency of the ASM gRNAs, we purified genomic DNA 24 hours following transfection of HaCaT cells with plasmids expressing Cas9 and either the G1 or G2 ASM gRNAs. We then used PCR primers to amplify the region of the ASM locus targeted for editing by Cas9 and the gRNAs. The PCR products were then heated and allowed to re-anneal to enable heteroduplex formation. The enzyme was then treated with T7 endonuclease which recognizes DNA mismatches present in heteroduplexes and cleaves the DNA. Thus, if the Cas9 enzyme was efficiently targeted by the guide RNAs to the ASM locus for genome editing, then PCR amplification of the locus should yield a mixture of products containing wild-type and mutant sequence that form a heteroduplex that can be cut by T7 endonuclease. PCR amplification of the ASM locus from genomic DNA of cells transfected with both gRNAs yielded an expect product of 371 bp (Figure 18). If the gRNAs efficiently targeted Cas9 to the ASM locus, then treatment with T7 endonuclease should yield products of G1 165 bp and 206 bp for the G1 gRNA and approximately 125 bp and 246 bp for the G2 gRNA. However, T7 endonuclease failed to generate DNAs of the expected sizes (Figure 19). These results indicate that the ASM gRNAs were not effective at targeting the Cas9 nuclease to the ASM locus for genome editing.

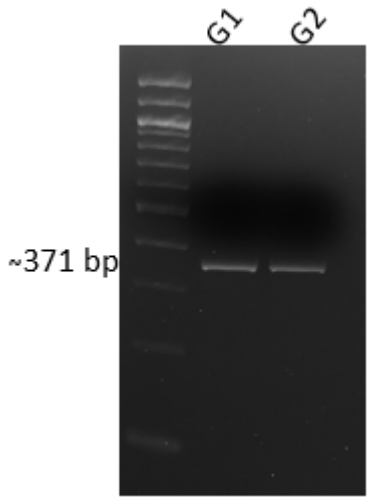

Figure 18: PCR amplification of the ASM

Amplification of the ASM locus from genomic DNA of cells transfected with both gRNAs (G1 and G2) yielded an expect product of 371 bp.

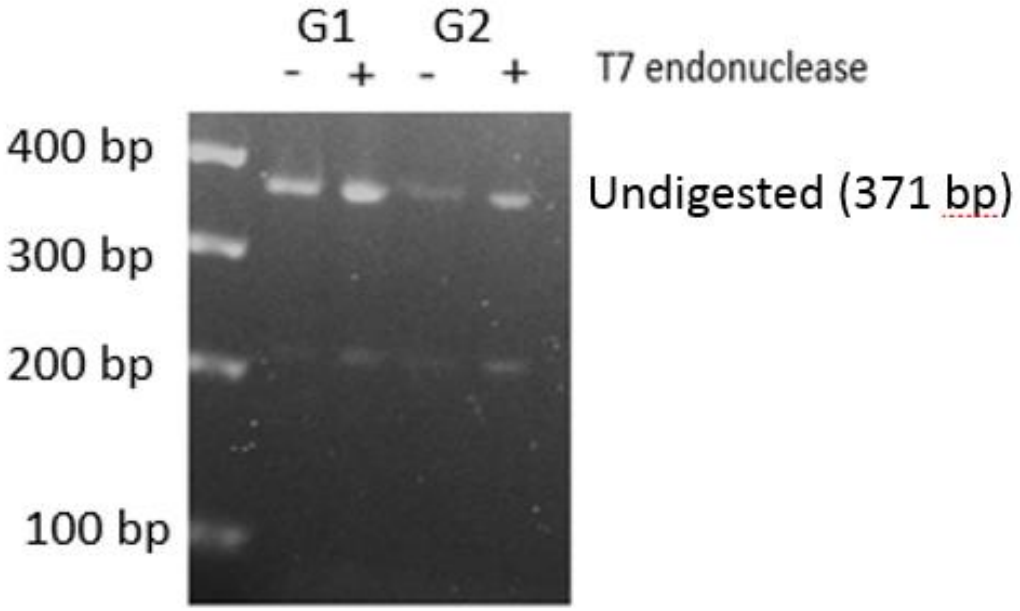

Figure 19:Genomic targeting efficiency of Cas9/gRNA with T7 Endonuclease 1

PCR result of using T7 to detect mutation at ASM target site. The resultant sizes of T7 endonuclease product G1 was approximately 206 bp. and G2 was approximately 246 bp. The cleaved sizes (165 bp and 125 bp) in both sample DNA was not observed from

the images taken from the agarose gel thus suggesting Cas9/gRNA could be inefficient in cutting the site of interest.

4.11 Comparison of MVP release in WT and ASM-KO NMF

Given that we were unsuccessful in generating HaCaT ASM KO cells, we sought an alternative strategy. We therefore derived primary fibroblasts (normal mouse fibroblasts, NMF) from the skin of new-born ASM-knockout mice for our studies. Fibroblast cells derived from both WT and ASM KO mice were treated with VEH, imipramine (IMI), CPAF, UVB, BURN, C2-ceramide and di-C2 (Figure 20) and incubated at 37°C for 4 hours. As shown in Figure 20, no significant difference in MVP release was observed between any treatment groups in the WT and ASM-KO NMF. Given that we found that fibroblasts did not respond positively to the various stressors, these studies indicate that fibroblasts may not be not an appropriate model.

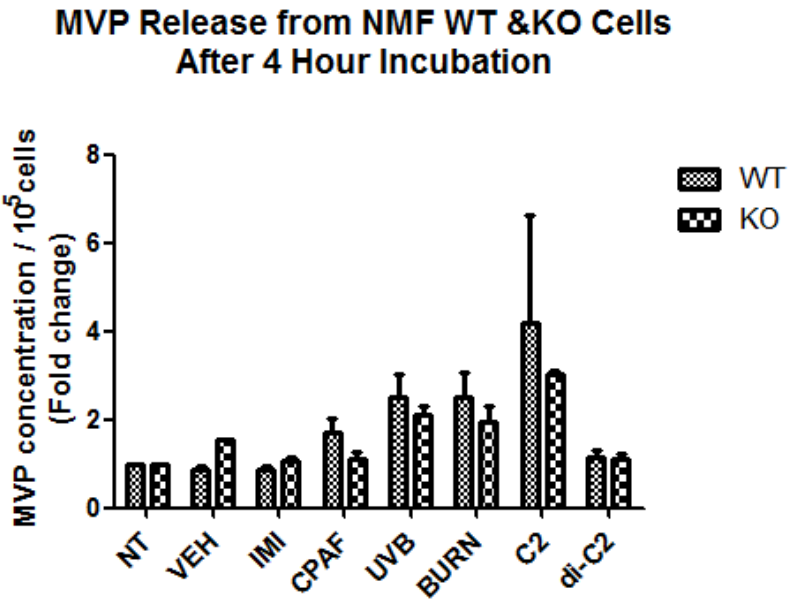

Figure 20: MVP release from NMF WT and ASM-KO primary skin fibroblasts

MVP release from NMF WT and ASM KO NMF has no significant difference in all treatment groups. The data represented are mean ± SEM MVP concentration per 100,000 cells (from 2 independent experiments). Groups were compared using two-way ANOVA. Differences in samples were considered significant if the P value was less than 0.05.

CHAPTER 5: DISCUSSION AND CONCLUSIONS

Ethanol is a known intoxicant. Both ethanol and ceramide activate ROS formation in part by activating apoptotic pathways, thus indicating the involvement of ceramide in ethanol-mediated apoptosis [54]. Thermal burn injury causes local effects at the sites of injury and could lead to systemic effects. *In vivo* studies using WT mice show that MVPs are found not just only in skin taken from affected the area but also in the serum which could possibly be shed from the epidermis. The mechanism by which this occurred is not clear, however, but the shedding of MVPs after exposure to stimuli is associated with cell to cell communication and this could be a possible means. To test if MVP release is dependent on PAFR, we exposed PAFR-KO mice to similar treatment to the WT mice. In PAFR-KO mice, there was no significant release of MVPs after TBI or EtOH exposure, which suggests that PAFR is involved in the generation of MVP *in vivo.*

In vitro studies using HaCaT cells demonstrated an increase in MVP release after exposure to EtOH alone. Combining EtOH with TBI resulted in an additive effect on MVP release. However, UVB + EtOH did not appear to exert greater effects than UVB alone. Treatment of HaCaT cells exposed to EtOH and TBI with imipramine resulted in a significant decrease in MVP release. However, treatment with imipramine had no significant effect on EtOH induced MVP release.

Attempt of knocking out ASM in HaCaT cells using CRISPR Cas9 genomic editing was not successful on analyzing several colonies using immuno-dot blot. When HaCaT cells transfected with Cas9 and ASM gRNAs were exposed to stressors that

induce MVPs and compared to normal, un-transfected HaCaT cells, the results obtained showed that the transfected cells responded to these stressors in a similar manner as in normal HaCaT cells. Commercially generated CRISPR Cas9 ASM-KO HAP1 cells obtained also responded to stressors in a similar manner as WT HAP1 cells. Thus, using two different cell types (HaCaT and HAP1) and three different guide RNAs (all targeting exon 1 of ASM), the CRISPR Cas9 failed to generate ASM-KO cells with defects in MVP release. Flow cytometry was also carried out to detect presence of ASM in HaCaT and cells transfected with CRISPR Cas9 complex upon treatment with CPAF and UVB. Result obtained showed similar florescence intensity detected in HaCaT cells.

To define the possibility that the gRNAs were not appropriate, we conducted direct testing using T7 endonuclease to determine the cutting efficiency of these gRNA. Results obtained showed inefficient gRNA cutting. We believe that this provides an explanation for why we were unable to effectively knockout the gene of interest in this study.

We also investigated the translocation of ASM to the outer leaflet of the plasma membrane at time 10 and 30 minutes incubation period after treatment with or with CPAF. ASM-stained cells treated with CPAF at 10 mins showed some spots (believed to be ASM) on the plasma membrane of the cells, while none were seen in the vehicle treated FITC staining. We also observed that the immunofluorescence staining by FITC had diminished at 30 minutes. This resulted suggest that the translocation of ASM from nucleus to the membrane occurs rapidly on exposure to various stimuli. Supporting the study carried out by Li *et al* [37].

The first limitation in this study is that the gRNAs were not efficient in cutting and deleting the gene of interest (ASM) in HaCaT cells. A specific and precise ASM-KO could support the idea of imipramine inhibited MVP release on exposure to UVB, BURN and CPAF. Use of confocal image will give a more defined image of ASM translocation to the outer leaflet of the membrane. The measurement of ASM activity using scintillation counter/HPLC to measure the production of ceramide would have also helped in this study.

Our obtaining ASM KO mice will assist in future studies defining the role of ASM in MVP release. Unfortunately, these mice have just come out of quarantine and we are only now able to grow primary cells from KO mice. Of importance, these mice are bred using heterozygous males and females which limits our ability to generate large numbers of mice.

Our current model is that upon environmental stressors, PAF is produced which then induces a rapid ASM translocation to the cell membrane. This process then facilitates MVP formation and release through ceramide formation. Our study provides evidence that ethanol induces MVP release in keratinocyte cells, skin, and serum from mice. It also proves that PAFR is necessary in the release of MVP on exposure to TBI. One area which will be of importance to assess is if the MVP found in skin and serum in mice are from keratinocytes. Our laboratory is currently screening keratinocyte-specific markers and it is our hope to be able to generate one to address this important question.

In summary, the present studies have unlocked a new effect of alcohol, namely, that EtOH can generate MVP. Since the role of MVP in skin-derived injury is unknown, this finding is of unclear significance at this time. However, an understanding

of how MVP production is regulated, such as possibly via ASM, could provide important tools to dissect the role of MVP in skin responses.

REFERENCES

[1] Faunce D 1998 Glucocorticoids protect against suppression of T cell responses in a murine model of acute ethanol exposure and thermal injury by regulating IL-6. *J. Leukoc.* **64** 724–32

[2] Fahy K, Liu L, Rapp C M, Borchers C, Bihl J C, Chen Y, Simman R and Travers J B 2017 Invited Review UVB-generated Microvesicle Particles : A Novel Pathway by Which a Skin-specific Stimulus Could Exert Systemic Effects *Photochemistry and Photobiology* **93** 937–942

[3] Mause S F and Weber C 2010 Microparticles: protagonists of a novel communication network for intercellular information exchange. *Circ. Res.* **107** 1047–57

[4] Distler H W, Pisetsky D S, Huber L C, Kalden J R, Gay S and Distler O 2005 Microparticles as Regulators of Inflammation Novel Players of Cellular Crosstalk in the Rheumatic Diseases **52** 3337–48

[5] Vion A-C, Ramkhelawon B, Loyer X, Chironi G, Devue C, Loirand G, Tedgui A, Lehoux S and Boulanger C M 2013 Shear stress regulates endothelial microparticle release. *Circ. Res.* **112** 1323–33

[6] Elovaara I, Lällä M, Spåre E, Lehtimäki T, Dastidar P, Mao W W, Horstman L L and Ahn Y S 1998 Methylprednisolone reduces adhesion molecules in blood and cerebrospinal fluid in patients with MS. *Neurology* **51** 1703–8

[7] Benedusi M, Frigato E, Beltramello M, Bertolucci C and Valacchi G 2018 Circadian clock as possible protective mechanism to pollution induced

keratinocytes damage *Mech. Ageing Dev.* **172** 13–20

[8] Bito T and Nishigori C 2012 Impact of reactive oxygen species on keratinocyte signaling pathways *Journal of Dermatological Science* **68** 3–8

[9] Marathe G K, Johnson C, Billings S D, Southall M D, Pei Y, Spandau D, Murphy R C, Zimmerman G A, Mcintyre T M, Travers J B and Roudebush R L 2005 Ultraviolet B Radiation Generates Platelet-activating Factor-like Phospholipids underlying Cutaneous Damage *J. Biol. Chem.* **280 (42)** 35448-57

[10] Sticozzi C, Cervellati F, Muresan X M, Cervellati C and Valacchi G 2014 Resveratrol prevents cigarette smoke-induced keratinocytes damage *Food Funct.* **5** 2348

[11] Bihl J C, Rapp C M, Chen Y and Travers J B 2016 UVB Generates Microvesicle Particle Release in Part Due to Platelet-activating Factor Signaling *Photochem Photobiol.* **92(3)** 503–506

[12] Sahu R P, Harrison K A, Weyerbacher J, Murphy R C, Konger R L, Garrett J E, Chin-Sinex H J, Johnston Ii M E, Dynlacht J R, Mendonca M, Mcmullen K, Li G, Spandau D F and Travers J B 2016 Radiation therapy generates platelet-activating factor agonists *Oncotarget* **7**

[13] Walterscheid J P, Ullrich S E and Nghiem D X 2002 Platelet-activating Factor, a Molecular Sensor for Cellular Damage, Activates Systemic Immune Suppression *J. Exp. Med* **00** 171–9

[14] Travers J B, Berry D, Yao Y, Yi Q, Konger R L and Travers J B Ultraviolet B 2010 Radiation of Human Skin Generates Platelet-activating Factor Receptor Agonists *Photochem. Photobiol.* **86 (4)** 949-54

[15] Dy L C, Pei Y and Travers J B 1999 Augmentation of ultraviolet B radiation-induced tumor necrosis factor production by the epidermal platelet-activating factor receptor. *J. Biol. Chem.* **274** 26917–21

[16] Yao Y, Wolverton J E, Zhang Q, Marathe G K, Al-Hassani M, Konger R L, Travers J B and Roudebush R L 2010 Ultraviolet B Radiation Generated Platelet-Activating Factor Receptor Agonist Formation Involves EGF-R-Mediated Reactive Oxygen Species 1 *Photochemistry and Photobiology* **86** 949–954

[17] Peus D, Vasa R A, Meves A, Pott M, Beyerle A, Squillace K and Pittelkow M R 1998 H2O2 Is an Important Mediator of UVB-Induced EGF-Receptor Phosphorylation in Cultured Keratinocytes *J. Invest. Dermatol.* **110** 966–71

[18] Countryman N B, Pei Y, Yi Q, Spandau D F and Travers J B 2000 Evidence for Involvement of the Epidermal Platelet- Activating Factor Receptor in Ultraviolet-B-Radiation- Induced Interleukin-8 Production *J Invest Dermatol.* **115** 267–272

[19] Kornhuber J, Tripal P, Reichel M, Terfloth L, Bleich S, Wiltfang J and Gulbins E 2008 Identification of New Functional Inhibitors of Acid Sphingomyelinase Using a Structure-Property-Activity Relation Model *J. Med. Chem.* **51** 219–237

[20] Ferlinz K, Hurwitz R, Vielhaber G, Suzukit K and Sandhoff K 1994 Occurrence of two molecular forms of human acid sphingomyelinase *Biochem. J* **301** 855–62

[21] McGovern M M, Wasserstein M P, Giugliani R, Bembi B, Vanier M T, Mengel E, Brodie S E, Mendelson D, Skloot G, Desnick R J, Kuriyama N and Cox G F 2008 A prospective, cross-sectional survey study of the natural history of Niemann-Pick disease type B. *Pediatrics* **122** e341-9

[22] Stancevic B and Kolesnick R 2010 Ceramide-rich platforms in transmembrane signaling *FEBS Lett.* **584** 1728–40

[23] Simonis A, Hebling S, Gulbins E, Schneider-Schaulies S and Schubert-Unkmeir A 2014 Differential activation of acid sphingomyelinase and ceramide release determines invasiveness of Neisseria meningitidis into brain endothelial cells. *PLoS Pathog.* **10** e1004160

[24] Münzer P, Borst O, Walker B, Schmid E, Feijge M A H, Cosemans J M E M, Chatterjee M, Schmidt E-M, Schmidt S, Towhid S T, Leibrock C, Elvers M, Schaller M, Seizer P, Ferlinz K, May A E, Gulbins E, Heemskerk J W M, Gawaz M and Lang F 2014 Acid sphingomyelinase regulates platelet cell membrane scrambling, secretion, and thrombus formation. *Arterioscler. Thromb. Vasc. Biol.* **34** 61–71

[25] Morelli A, Chiozzi P, Chiesa A, Ferrari D, Sanz J M, Falzoni S, Pinton P, Rizzuto R, Olson M F and Di Virgilio F 2003 Extracellular ATP causes ROCK I-dependent bleb formation in P2X7-transfected HEK293 cells. *Mol. Biol. Cell* **14** 2655–64

[26] Bianco F, Perrotta C, Novellino L, Francolini M, Riganti L, Menna E, Saglietti L, Schuchman E H, Furlan R, Clementi E, Matteoli M and Verderio C 2009 Acid sphingomyelinase activity triggers microparticle release from glial cells *EMBO J.* **28** 1043–54

[27] Angela Dolganiuc, M.D. P D Alcohol and Viral Hepatitis: Role of Lipid Rafts 2015 *Alcohol Res.* **37 (2)** 299-309

[28] Longato L, Ripp K, Setshedi M, Dostalek M, Akhlaghi F, Branda M, Wands J R and De La Monte S M 2012 Insulin Resistance, Ceramide Accumulation, and

Endoplasmic Reticulum Stress in Human Chronic Alcohol-Related Liver Disease *Oxid. Med. Cell. Longev.* **479348**

[29] Liangpunsakul S, Sozio M S, Shin E, Zhao Z, Xu Y, Ross R A, Zeng Y and Crabb D W 2010 Inhibitory effect of ethanol on AMPK phosphorylation is mediated in part through elevated ceramide levels *Am. J. Physiol. Liver Physiol.* **298** G1004–12

[30] Viktorov A V. and Yurkiv V A 2008 Effects of Ethanol and Lipopolysaccharide on the Sphingomyelin Cycle in Rat Hepatocytes *Bull. Exp. Biol. Med.* **146** 753–5

[31] Lawler J F, Yin M, Diehl A M, Roberts E and Chatterjee S 1998 Tumor necrosis factor-alpha stimulates the maturation of sterol regulatory element binding protein-1 in human hepatocytes through the action of neutral sphingomyelinase. *J. Biol. Chem.* **273** 5053–9

[32] Mühle C, Huttner H B, Walter S, Reichel M, Canneva F, Lewczuk P, Gulbins E and Kornhuber J 2013 Characterization of Acid Sphingomyelinase Activity in Human Cerebrospinal Fluid ed L J Siskind *PLoS One* **8** e62912

[33] Liangpunsakul S, Rahmini Y, Ross R A, Zhao Z, Xu Y and Crabb D W 2012 Imipramine blocks ethanol-induced ASMase activation, ceramide generation, and PP2A activation, and ameliorates hepatic steatosis in ethanol-fed mice *Am. J. Physiol. Liver Physiol.* **302** G515–23

[34] Karabeyog M, Lu ˘, Lent Nal B, Bozkurt B L, Dolapçı I, Bilgihan A, Karabeyog I and Cengiz M 2008 The Effect of Ethyl Pyruvate on Oxidative Stress in Intestine and Bacterial Translocation After Thermal Injury *Journal of Surgical Research* **144** 59–63

[35] Harrison K A, Romer E, Weyerbacher J, Ocana J A, Sahu R P, Murphy R C, Kelly L E, Smith T A, Rapp C M, Borchers C, Cool D R, Li G, Simman R and Travers J B 2018 Enhanced Platelet-activating Factor synthesis facilitates acute and delayed effects of ethanol intoxicated thermal burn injury. *J. Invest. Dermatol.* **0**

[36] Charruyer A, Grazide S, Bezombes C, Müller S, Laurent G and Jaffrézou J-P 2005 UV-C light induces raft-associated acid sphingomyelinase and JNK activation and translocation independently on a nuclear signal. *J. Biol. Chem.* **280** 19196–204

[37] Li X, Gulbins E and Zhang Y 2012 OXIDATIVE STRESS TRIGGERS CA 2+ -DEPENDENT LYSOSOME TRAFFICKING AND ACTIVATION OF ACID SPHINGOMYELINASE *Cell Physiol Biochem* **30(4)** 815–826

[38] Rodríguez A, Webster P, Ortego J and Andrews N W 1997 Lysosomes behave as Ca2+-regulated exocytic vesicles in fibroblasts and epithelial cells. *J. Cell Biol.* **137** 93–104

[39] Smart E J, Graf G A, Mcniven M A, Sessa W C, Engelman J A, Scherer P E, Okamoto T and Lisanti M P 1999 MINIREVIEW Caveolins, Liquid-Ordered Domains, and Signal Transduction OVERVIEW: CAVEOLAE AND CAVEOLA-RELATED DOMAINS ARE LIQUID-ORDERED MICRODOMAINS *MOLECULAR AND CELLULAR BIOLOGY* **19** 7289–304

[40] Cong L, Ran F A, Cox D, Lin S, Barretto R, Habib N, Hsu P D, Wu X, Jiang W, Marraffini L A and Zhang F 2013 Multiplex Genome Engineering Using CRISPR/Cas Systems *Science (80-.).* **339** 819–23

[41] Ishino Y, Shinagawa H, Makino K, Amemura M and Nakata A 1987 Nucleotide

Sequence of the iap Gene, Responsible for Alkaline Phosphatase Isozyme Conversion in Escherichia coli, and Identification of the Gene Product *J. Bacteriol.* **169** 5429–33

[42] Garneau J E, Dupuis M-È, Villion M, Romero D A, Barrangou R, Boyaval P, Fremaux C, Horvath P, Magadán A H and Moineau S 2010 The CRISPR/Cas bacterial immune system cleaves bacteriophage and plasmid DNA *Nature* **468** 67–71

[43] Jinek M, Chylinski K, Fonfara I, Hauer M, Doudna J A and Charpentier E 2012 A Programmable Dual-RNA—Guided DNA Endonuclease in Adaptive Bacterial Immunity *Source Sci. New Ser.* **337** 816–21

[44] O 'connell M R, Oakes B L, Sternberg S H, East-Seletsky A, Kaplan M and Doudna J A 2014 Programmable RNA recognition and cleavage by CRISPR/Cas9 *Nature* **516(7530)** 263–266

[45] Thomas K R, Folger K R and Capecchi M R 1986 High frequency targeting of genes to specific sites in the mammalian genome *Cell* **44** 419–28

[46] Mansour S L, Thomas K R and Capecchi M R 1988 Disruption of the proto-oncogene int-2 in mouse embryo-derived stem cells: a general strategy for targeting mutations to non-selectable genes *Nature* **336** 348–52

[47] Zhang H and Mccarty N 2016 CRISPR-Cas9 technology and its application in haematological disorders *Br J Haematol.* **175(2)** 208–225

[48] Huang X, Wang Y, Yan W, Smith C, Ye Z, Wang J, Gao Y, Mendelsohn L and Cheng L 2015 Production of Gene-Corrected Adult Beta Globin Protein in Human Erythrocytes Differentiated from Patient iPSCs After Genome Editing

of the Sickle Point Mutation *Stem Cells* **33** 1470–9

[49] Manabu Soda Y L C, Munehiro Enomoto S T, Yoshihiro Yamashita, Shunpei Ishikawa, Shin-ichiro Fujiwara, Hideki Watanabe, Kentaro Kurashina, Hisashi Hatanaka, Masashi Bando, Shoji Ohno Y I, Hiroyuki Aburatani T N, Yasunori Sohara and Yukihiko Sugiyama & Hiroyuki Mano Identification of the transforming EML4-ALK fusion gene in non-small-cell l...: EBSCOhost

[50] Reardon S 2016 Welcome to the CRISPR zoo *Nature* **531** 160–3

[51] Ablain J, Durand E M, Yang S, Zhou Y and Zon L I 2015 A CRISPR/Cas9 Vector System for Tissue-Specific Gene Disruption in Zebrafish *Dev. Cell* **32** 756–64

[52] Boukamp P, Chen J, Gonzales F, Jones P A and Fusenig N E 1992 Progressive stages of "transdifferentiation" from epidermal to mesenchymal phenotype induced by MyoD1 transfection, 5-aza-2'-deoxycytidine treatment, and selection for reduced cell attachment in the human keratinocyte line HaCaT. *J. Cell Biol.* **116** 1257–71

[53] Krishma Halai Mouse Skin Fibroblast Isolation 2016 http://www.ukrmp.org.uk/wp-content/uploads/2017/08/Mouse-Skin-Fibroblast-Isolation.pdf

[54] Anon CRISPR/Cas9 Genome Editing Application Guide https://cdn.origene.com/assets/documents/crispr-cas9/crispr_manual.pdf

[55] Saito M and Saito M 2013 Involvement of Sphingolipids in Ethanol Neurotoxicity in the Developing Brain *Brain Sci* **3** 670–703